



RESEARCH ARTICLE

10.1029/2022JG007252

†Deceased 4 January 2022.

Key Points:

- Genetic signals of marine prokaryotes and eukaryotes change considerably from surface to deep waters and into the sediments
- DNA of surface-dwelling organisms in a deep water column degrades while sinking with little DNA preserved in the sediments
- Organisms that are well represented in deeper waters appear to have a higher likelihood of becoming preserved in the sediments

Supporting Information:

Supporting Information may be found in the online version of this article.

Correspondence to:

L. Armbrecht,
linda.armbrecht@utas.edu.au

Citation:

Armbrecht, L., Focardi, A., Lawler, K.-A., O'Brien, P., Leventer, A., Noble, T. L., et al. (2023). From the surface ocean to the seafloor: Linking modern and paleo-genetics at the Sabrina Coast, East Antarctica (IN2017_V01). *Journal of Geophysical Research: Biogeosciences*, 128, e2022JG007252. <https://doi.org/10.1029/2022JG007252>

Received 19 OCT 2022

Accepted 13 MAR 2023













Author Contributions:

Conceptualization: Linda Armbrecht, Amaranta Focardi, Kelly-Anne Lawler
Data curation: Linda Armbrecht, Amaranta Focardi, Kelly-Anne Lawler, Amy Leventer, Taryn L. Noble, Bradley Opdyke, Meghan Duffy, Adrián López-Quirós, Leanne Armand
Formal analysis: Linda Armbrecht, Amaranta Focardi, Kelly-Anne Lawler

© 2023 The Authors.

This is an open access article under the terms of the [Creative Commons Attribution-NonCommercial License](https://creativecommons.org/licenses/by/4.0/), which permits use, distribution and reproduction in any medium, provided the original work is properly cited and is not used for commercial purposes.

From the Surface Ocean to the Seafloor: Linking Modern and Paleo-Genetics at the Sabrina Coast, East Antarctica (IN2017_V01)

Linda Armbrecht¹ , Amaranta Focardi² , Kelly-Anne Lawler³ , Phil O'Brien³ , Amy Leventer⁴ , Taryn L. Noble¹ , Bradley Opdyke³ , Meghan Duffy⁵, Dimitris Evangelinos⁶ , Simon C. George⁷ , Jan Lieser¹ , Adrián López-Quirós^{8,9} , Alix Post¹⁰ , Martin Ostrowski², Ian Paulsen⁷, and Leanne Armand^{3,†}

¹Institute for Marine and Antarctic Studies, University of Tasmania, Battery Point, TAS, Australia, ²Climate Change Cluster, University of Technology Sydney, Ultimo, NSW, Australia, ³Research School of Earth Sciences, Australian National University, Acton, ACT, Australia, ⁴Department of Geology, Colgate University, Hamilton, NY, USA, ⁵Department of Geology, University of Otago, Dunedin, New Zealand, ⁶Department of Earth and Ocean Dynamics, University of Barcelona, Barcelona, Spain, ⁷School of Natural Sciences, Macquarie University, Sydney, NSW, Australia, ⁸Department of Stratigraphy and Paleontology, University of Granada, Granada, Spain, ⁹Department of Geoscience/iCLIMATE Centre, Aarhus University, Aarhus C, Denmark, ¹⁰Marine and Antarctic Geoscience, Geoscience Australia, Symonston, ACT, Australia

Abstract With ongoing climate change, research into the biological changes occurring in particularly vulnerable ecosystems, such as Antarctica, is critical. The Totten Glacier region, Sabrina Coast, is currently experiencing some of the highest rates of thinning across all East Antarctica. An assessment of the microscopic organisms supporting the ecosystem of the marginal sea-ice zone over the continental rise is important, yet there is a lack of knowledge about the diversity and distribution of these organisms throughout the water column, and their occurrence and/or preservation in the underlying sediments. Here, we provide a taxonomic overview of the modern and ancient marine bacterial and eukaryotic communities of the Totten Glacier region, using a combination of 16S and 18S rRNA amplicon sequencing (modern DNA) and shotgun metagenomics (sedimentary ancient DNA, *seDaDNA*). Our data show considerable differences between eukaryote and bacterial signals in the water column versus the sediments. Proteobacteria and diatoms dominate the bacterial and eukaryote composition in the upper water column, while diatoms, dinoflagellates, and haptophytes notably decrease in relative abundance with increasing water depth. Little diatom *seDaDNA* is preserved in the sediments, which are instead dominated by Proteobacteria and Retaria. We compare the diatom microfossil and *seDaDNA* record and link the weak preservation of diatom *seDaDNA* to DNA degradation while sinking through the water column to the seafloor. This study provides the first assessment of DNA transfer from ocean waters to sediments and an overview of the microscopic communities occurring in the climatically important Totten Glacier region.

Plain Language Summary Antarctica is highly vulnerable to climate change and research into how marine organisms around the continent will respond to warming conditions is important. Microscopic organism, such as bacteria and phytoplankton, are key in the marine ecosystems because they support the entire marine food web. In this study, we investigated the composition of these microorganisms in the climatically important East Antarctic Totten Glacier region. We profiled compositional changes throughout the water column and into underlying seafloor sediments, which provided information on both actively living and long dead organisms, and thus modern and past environmental conditions, respectively. We used genetic techniques to compare these marine communities, focusing on the taxonomically informative small subunit ribosomal ribonucleic acid (SSU rRNA) gene. Our study provides an overview about the microorganisms that live in the modern ocean in the Totten Glacier region, and how well their genetic signatures preserve in the underlying sediments. This knowledge is important both for assessments of present-day marine ecosystem health and functioning, and when reconstructing past ocean environments as analogs to ongoing climate change.

Funding acquisition: Linda Armbrecht, Amaranta Focardi, Phil O'Brien, Taryn L. Noble, Alix Post, Ian Paulsen, Leanne Armand

Investigation: Linda Armbrecht, Amaranta Focardi, Kelly-Anne Lawler, Phil O'Brien, Amy Leventer, Taryn L. Noble, Bradley Opdyke, Meghan Duffy, Dimitris Evangelinos, Simon C. George, Adrián López-Quirós, Alix Post, Leanne Armand

Methodology: Linda Armbrecht, Amaranta Focardi, Kelly-Anne Lawler, Amy Leventer, Taryn L. Noble, Bradley Opdyke, Meghan Duffy

Project Administration: Linda Armbrecht, Amaranta Focardi, Phil O'Brien, Alix Post, Leanne Armand

Resources: Linda Armbrecht, Amaranta Focardi, Kelly-Anne Lawler, Phil O'Brien, Amy Leventer, Taryn L. Noble, Bradley Opdyke, Meghan Duffy, Jan Lieser, Adrián López-Quirós, Martin Ostrowski, Leanne Armand

Software: Linda Armbrecht, Amaranta Focardi, Kelly-Anne Lawler

Supervision: Phil O'Brien, Martin Ostrowski, Ian Paulsen, Leanne Armand

Validation: Linda Armbrecht, Amaranta Focardi, Kelly-Anne Lawler, Taryn L. Noble, Bradley Opdyke

Visualization: Kelly-Anne Lawler, Jan Lieser, Adrián López-Quirós

Writing – original draft: Linda Armbrecht, Amaranta Focardi, Kelly-Anne Lawler

Writing – review & editing: Linda Armbrecht, Amaranta Focardi, Kelly-Anne Lawler, Phil O'Brien, Amy Leventer, Taryn L. Noble, Bradley Opdyke, Meghan Duffy, Dimitris Evangelinos, Simon C. George, Jan Lieser, Adrián López-Quirós, Alix Post, Leanne Armand

1. Introduction

Polar regions are particularly vulnerable to climate change. The latest Intergovernmental Panel on Climate Change (IPCC) models have predicted that the Arctic and Antarctic are warming faster than tropical regions under 1.5°C, 2°C, and 4°C global temperature increase scenarios (IPCC, 2021). Around Antarctica, large-scale alterations in Southern Ocean circulation and environmental conditions have already been shown, as has their influence at all levels of the Antarctic marine food web (Rogers et al., 2020). These impacts on Antarctic marine organisms differ regionally (Rogers et al., 2020) and are usually associated with sea-ice characteristics and/or seasonal dynamics (Constable et al., 2014). Rising Southern Ocean temperatures are already driving the poleward range expansion of organisms adapted to thrive in cold temperature oceanographic conditions (e.g., phyto- and zooplankton; Constable et al., 2014; McLeod et al., 2012). Moreover, increasing ocean acidification impacts the survival of calcifying organisms such as coccolithophores, and the reproductive success of zooplankton such as Antarctic krill (Constable et al., 2014; Kawaguchi et al., 2011, and references therein). Consequently, these “lower food web” changes may impact species at higher trophic levels, including marine predators (Constable et al., 2014).

A particularly important study region in the context of rapid, climate-change-induced ecosystem changes is the Sabrina Coast, East Antarctica. This coast is bounded by the Dalton Ice Tongue to the east (~125°E) and the Totten Glacier to the west (~115°E). The Totten Glacier, which drains ice in the Aurora Subglacial Basin, drains more ice than any other East Antarctic Ice Sheet glacier (Greenbaum et al., 2015). Significant retreat of the grounding line (1–3 km) and ice thinning (on average 0.7 ± 0.1 m/year) have been observed between 1996 and 2013 (Li et al., 2015). The Sabrina Coast is located within the Wilkes Land coastland, which has been shown to have lost a considerable amount of ice (51 ± 13 Gt/year) between 1979 and 2017, with East Antarctica to be a dominant contributor to global sea level rise (4.4 ± 0.9 mm) during the same time period (Rignot et al., 2019).

The main water masses over the continental rise of the Totten Glacier region are Antarctic Surface Water (occurs at approximately 0–50 m water depth and is characterized by temperatures of $>-1.5^\circ\text{C}$ and salinities <34.2 S), Winter Water (approximately 50–400 m; -1.92°C to 1.75°C , 34.0–34.5 S), and modified Circumpolar Deep Water (mCDW, below ~400 m, $>0^\circ\text{C}$, >34.5 S; Bensi et al., 2022). Antarctic Bottom Water (temperature -0.5°C to 0°C , salinity 34.63–34.67 S) occurs below ~2,000 m and is a mixture of remnant Ross Sea Bottom Water and Adélie Land Bottom Water. Bensi et al. (2022) report that, especially in the western Totten Glacier region (115°–117°E), intrusions of mCDW (e.g., triggered by wind-driven upwelling) onto the continental shelf are possible in areas where the shelf break is deeper than 400 m, as here mCDW can flow down the landward-sloping continental shelf, reaching the Totten Glacier grounding zone, and contributing to basal ice melt (as has been reported previously, e.g., Silvano et al., 2019). It has been suggested that the spatial distribution of the water masses is linked to the complex morphology of the seabed including several deep canyons in the Totten Glacier region (O'Brien et al., 2020). Additionally, the Sabrina Coast exhibits a unique and distinct benthic biodiversity on the shelf and upper slope (Post et al., 2017, 2020). However, an evaluation of water column biodiversity, as well as paleo-diversity of the sedimentary record, is still missing in this region.

The analyses of DNA signatures in the environment are increasingly applied to monitor modern and paleo-ocean biodiversity, respectively (Capo et al., 2022; Garlapati et al., 2019). The study of modern biodiversity usually involves filtering a few liters of sample water onto a sterile filter paper, extracting DNA from this filter, and then either analyzing all DNA in that sample (“shotgun” metagenomic approach), or the amplification and sequencing of genes of interest (metabarcoding approach; e.g., taxonomic marker genes, which can provide information on a sample’s taxonomic composition). Equivalent techniques in paleo-science are sedimentary ancient DNA analyses (*sedDNA*), where DNA is extracted from a few grams of sediment, and shotgun sequenced or enriched for target genes to study specific organisms (e.g., using hybridization capture techniques; e.g., Armbrecht, Hallegraef, et al., 2021; Armbrecht et al., 2022; Giosan et al., 2018; Orsi et al., 2017). While these *sedDNA* techniques allow the detection of soft-bodied organisms beyond the fossil record, analyses can be challenging as the acquired sequences are typically very degraded and short (<100 base pairs [bp]), resulting in possible misidentifications when comparing them to modern reference sequences (Armbrecht, 2020; Capo et al., 2022). Both modern DNA and *sedDNA* are reliant on the availability of high-quality reference sequences to prevent misidentification and/or reference bias (Armbrecht, Eisenhofer, et al., 2021; L. J. Clarke et al., 2021; Cowart et al., 2018).

It is thought that *sedDNA* is best preserved in organic-rich, non-UV exposed, anoxic, and cold environments (Armbrecht et al., 2019; Capo et al., 2022), hence, polar, deep ocean sediments are particularly suitable

for *sedaDNA*-based paleo-ecosystem studies. Indeed, eukaryote *sedaDNA* has been recovered from up to ~140,000-year-old sediments in the Arctic (De Schepper et al., 2019; Pawłowska et al., 2020; Zimmermann et al., 2020) and ~1 million-year-old sediments in the Antarctic (Armbrecht et al., 2022). However, even in “ideal” cold and low-oxygen conditions, genetic information is lost throughout the water column, for example, by postmortem DNA fragmentation, degradation, uptake of DNA by living organisms, and virus/bacteriophage activity (e.g., Corinaldesi et al., 2007; Thomsen & Willerslev, 2015; Wei et al., 2022). These processes continue in the sediment column, where taphonomic processes, and possibly species-specific degradation rates, may further impact the compositional profiles generated through *sedaDNA* analyses (Giguët-Covex et al., 2019). Determining the factors and rates of genetic information loss from water into sediments are important considerations when using *sedaDNA* to reconstruct paleo-environments (Barrenechea Angeles et al., 2020; Pawłowska et al., 2014).

In this study, we use both a modern and a paleo-genomics approach to investigate vertical profiles of marine organisms (bacteria and eukaryotes) through the water column and underlying sediments at three sampling stations off the Sabrina Coast, East Antarctica. Water and sediment samples were collected during the “Sabrina Seafloor Survey” (IN2017_V01) and represent the surface waters, chlorophyll maximum depth, bottom waters, and several depths below the seafloor. Our aim is to provide the first biodiversity assessment of microorganisms in this region using modern DNA and *sedaDNA* techniques, and to investigate potential taxonomic information loss from the water to the sediments, using data collected at the same sampling locations during the same voyage.

2. Methods

2.1. Sample and Data Collection During IN2017_V01

Conductivity–temperature–depth (CTD) data, seawater samples, and sediment cores (Kasten Cores [KCs]) were collected during the *RV Investigator* voyage IN2017_V01 (“Sabrina Seafloor Survey”) between January and March 2017. Onboard sampling strategies and initial descriptions of sediment cores and samples have been described in detail by Armand et al. (2018) and are briefly summarized below. In this study, we focused on three sites, CTD03/KC02, CTD05/KC14, and CTD16/KC06 (from west to east, Figure 1 and Table 1).

2.2. IN2017_V01 Water Column Sampling

CTD profiles were collected at the three sites using a SBE911plus CTD (Seabird electronics) fitted with additional sensors (fluorescence, oxygen, turbidity, and altimeter). During the upward cast, seawater was collected from different depths (surface [0–8 m], chlorophyll *a* maximum depth [“chl max,” 45–90 m], below the chl max [95–140 m], and bottom [below 2,000 m], Table 1), using 12 L Niskin bottles (Ocean Test Equipment, Florida) mounted on a SBE11 rosette (CTD fluorescence data are publicly available at: https://www.cmar.csiro.au/data/trawler/dataset.cfm?survey=IN2017%5FV01&data_type=ctd). For the analysis of the microbial communities, 2 L of seawater were filtered onto a 0.2 μm pore diameter PES Sterivex filter (Millipore), and the filter was then stored at -80°C until further analysis on shore. Concomitantly, Niskin bottle seawater samples were analyzed onboard for nutrients (NO_x , PO_4 , Si), temperature, salinity, and dissolved oxygen from the same depths. Results from temperature, salinity, and dissolved oxygen were used to calibrate the results obtained from the CTD and CTD fitted sensors. Data and methodology for the physical and chemical analyses are available through the CSIRO Ocean and Atmosphere data trawler repository (https://www.cmar.csiro.au/data/trawler/survey_details.cfm?survey=IN2017_V01).

2.3. IN2017_V01 Sediment Core Collection and Supplementary Core Data Generation

Three gravity cores were collected using the Kasten Coring system (KC02, 2,161 m water depth, 2.4 m long; KC14, 2,100 m water depth, 3.4 m long; KC06, 3,361 m water depth, 2.7 m long; Figure 1 and Table 1). KC02 and KC14 were collected in the west of the survey region on the crest of submarine levees, while in the east, KC06 was collected ~1,200 m deeper at the bottom of Jeffrey Canyon. Upon core retrieval and opening, the core lithology was described including sediment color as per the Munsell Color Chart, sedimentary textures (e.g., grain size, dropstones, and mud clots), sharp or gradational contacts between color or lithology types, sedimentary structures (e.g., presence of laminations, bioturbation), and visible fossils (Armand et al., 2018). Coarse sediment fractions were separated by sieving the wet samples through a 63 μm sieve, and photographed onboard, using a camera-fitted stereomicroscope (1.5–6X magnification; Armand et al., 2018).

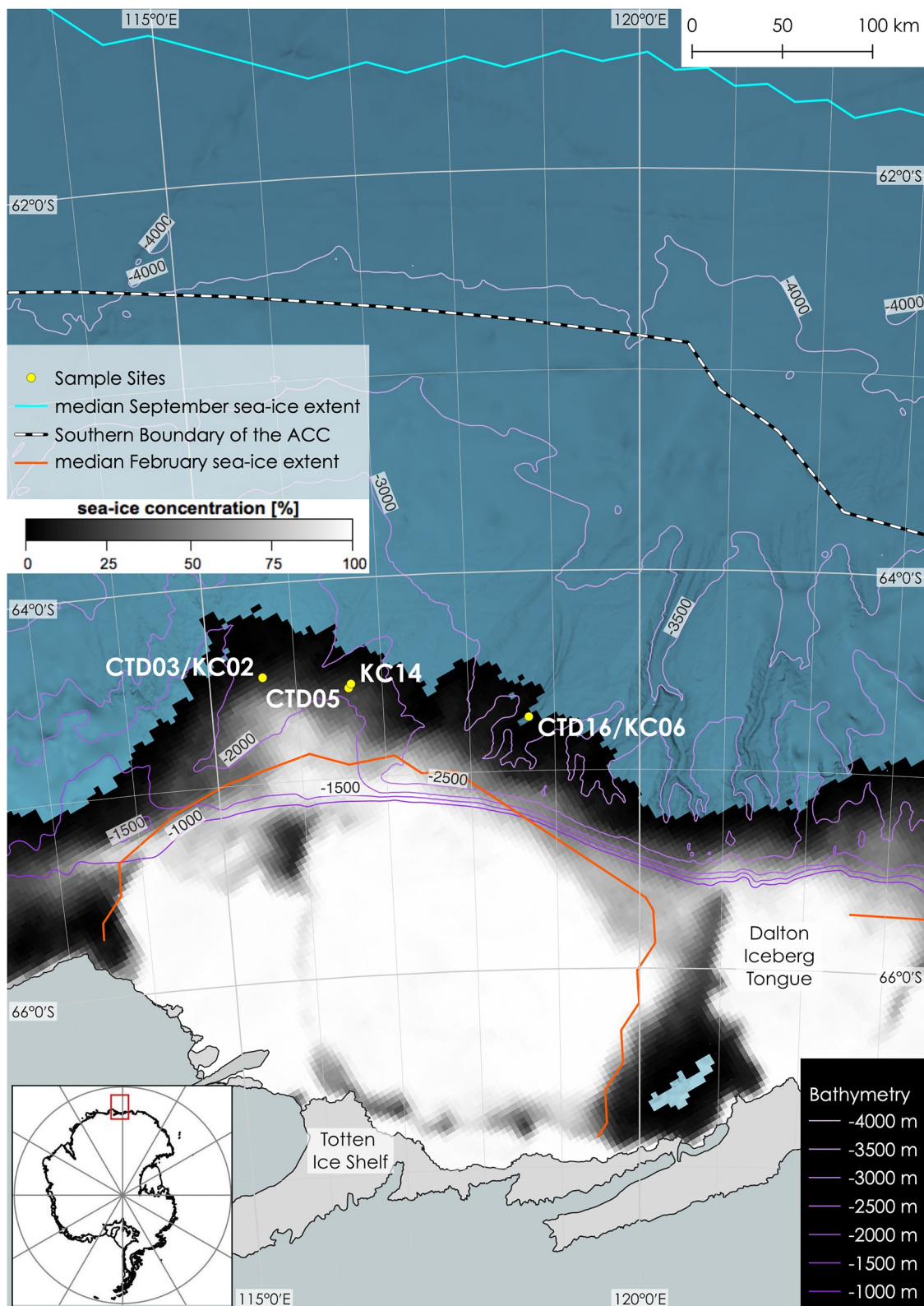


Figure 1. Sampling locations. Map of the sampling sites on the Sabrina Coast of Antarctica. Depicted are the median September sea-ice extent (light blue), southern boundary of the Antarctic Circumpolar Current (ACC; black/white), and median February sea-ice extent (red). For sampling depths in the water column and sediment, see Table 1. Satellite data: AMSR-2 sea-ice concentration data averaged for February 2017; data courtesy ICDC, University Hamburg. Sea-ice extent data were retrieved from the National Snow and Ice Data Center repository and are based on >15% sea-ice concentration (Fetterer et al., 2017). Bathymetry data and background are from IBCSO v2 (Dorschel et al., 2022).

Table 1
Sampling Location Details

Latitude (S)	Longitude (E)	Depth (m)	CTD cast	Water sample depths (m)	Sediment core	Sediment sample depths (cm)
64.47	115.62	2,161	CTD03	0: surface	KC02	210–211.5
				50: chl max		230–231.5
				110: below chl max		
				2,160: bottom		
64.73	118.7	3,361	CTD16	0: surface	KC06	0
				50: chl max		12–13.5
				125: below chl max		66–67.5
				3,361: bottom		110–111.5
						170–171.5
						260–261.5 A, B
64.55	116.61	2,104	CTD05 ^a	0: surface	n/a	
				85: chl max		
				140: below chl max		
				2,104: bottom		
64.53	116.64	2,100	n/a		KC14 ^a	40–41.5
						210–211.5
						330–331.5

Note. Listed are the exact coordinates of the sampling sites and the corresponding conductivity–temperature–depth (CTD) and Kasten Core (KC) locations, as well as depths sampled in the water column and sediment. Sediment depth intervals are provided, however, for simplification we refer to the top depth of this interval in the text hereafter. Chl max, chlorophyll *a* maximum depth.

^aKC14 and CTD05 were not collected at the same site, however, were in proximity of each other (see coordinates and Figure 1).

Postvoyage, detailed geochemical analyses were undertaken on selected cores. Elemental composition of the cores was determined via scanning X-ray fluorescence (XRF) using the Cox Analytical System ITRAX Core Scanner at the Australia Nuclear Science and Technology Organisation (ANSTO), Sydney. XRF measurements were made at 0.5 cm resolution with a Cr–He tube at 30 kV for semiquantitative Al and Si abundances. The XRF data were processed by removing any signals with an intensity lower than a threshold of 35,000 kcps. Magnetic susceptibility was measured at 0.1 cm resolution. Biogenic silica concentrations for KC14 (Tooze et al., 2020) were analyzed by Quickchem 8500 Series 2 FIA at the University of Tasmania. Diatom analyses were conducted on slides prepared using a random settling technique (Warnock & Scherer, 2015) and include both absolute and relative abundance determinations, based on diatom counts performed at 1,000X magnification. The geochemistry and diatom data are provided in Tables S2 and S3 in Supporting Information S1, respectively.

2.4. Age Control

Age models for KC02 and KC14 were developed by radiocarbon dating of the acid insoluble organic matter fraction by Accelerator Mass Spectrometry by DirectAMS (USA). The sediment samples (2–3 g) were pretreated prior to dating using equipment sterilized in a kiln at 450°C. Oven-dried (60°C) sediment samples were ground and leached in 2 M HCl on a hot block at 80°C for several hours to remove any carbonates present, followed by several Milli-Q water rinses to remove residual acid, before being dried in an oven (60°C). The KC14 dates were presented in Tooze et al. (2020). Two dates from the bottom of KC02 that are presented here (Figure 3 and Table S2 in Supporting Information S1) were corrected for old, recycled carbon contamination using the surface acid insoluble organic matter age in the multicore collected at the KC02 station (Creac’h et al., 2023) and calibrated using the Marine20 calibration curve (Heaton et al., 2020) in MatCal 2.41 (Lougheed & Obrochta., 2016). Due to the spatial variability in the reservoir age particularly around Antarctica, a reservoir correction for the glacial

aged KC02 sediments was applied using the difference between a regional Southern Ocean reservoir age at 22 ka (Skinner et al., 2019) and the Marine20 global mean reservoir age. For KC06, an age model is not yet fully established, with the oldest sediments potentially being from the Holocene or Last Interglacial (see Section 3 and Notes 1 and Table S2 in Supporting Information S1).

2.5. *seda*DNA Sample Collection

*Seda*DNA samples were collected using clean procedures (wearing two pairs of gloves, where the top pair was changed immediately when contaminated with sediment; limiting movement in a closed-door sampling room to create a still-air environment; Armbrrecht et al., 2019). Upon KC retrieval and opening, the outer, 0.5 cm of sediment exposed along the length of the core was removed by scraping in a perpendicular fashion with clean spatulas (pretreated with 3% bleach and 70% ethanol), working from the bottom to the top of the core. Plunge samples were collected by pushing sterile (gamma-irradiated) bottomless 15 mL centrifuge tubes (Falcon) into the sediment, generating a sample interval of 1.5 cm due to the size of the tube opening (hereafter, we refer to the top depth of this interval for simplicity). The tubes were transferred into a sterile plastic bag (WhirlPak), flash-frozen in liquid nitrogen (KC02, KC06) or at -80°C (KC14, which was taken later in the voyage when the liquid nitrogen supply was depleted). The samples were stored at -80°C until 2018, then at -20°C (the now recommended long-term storage temperature; Armbrrecht et al., 2019; Capo et al., 2021). Between two and six *seda*DNA samples per site were analyzed for this study to investigate different sediment types, depths, and locations (Table 1). At site KC06, we expected high diatom *seda*DNA yield, therefore analyzed a comparatively larger number of samples from this core (total of six depths with a duplicate sample of the bottom-most depth).

2.6. Modern DNA Extraction and Sequencing

DNA was extracted from the Sterivex filters using a commercial kit (Power water, QIAGEN) following the manufacturer's recommendation. DNA quality and quantity were assessed using a Nanodrop 2000 Spectrophotometer and a picogreen assay (both Thermofisher), respectively. Amplicon sequencing was undertaken for the V1–V3 region of the 16S rRNA gene (27f–519r) and V4 region of the 18S rRNA, respectively. PCR amplifications for both marker genes and libraries preparation using the Nextera XT index kit (Illumina) were carried out at the Ramaciotti Centre for Genomics (UNSW, Sydney), as outlined in the Australian Microbiome Marine Microbes methods SOP for 16S amplicons (<https://data.bioplatforms.com/organization/pages/australian-microbiome/methods>). The libraries were then sequenced on a MiSeq platform (Illumina), using pair-end sequencing for both 16S rRNA (300 bp reads) and 18S rRNA (250 bp) amplicons at the Ramaciotti Centre for Genomics.

2.7. Bioinformatic Analysis of Modern DNA in the Water Column

Cutadapt (Martin, 2011) was used to remove the adapters and primers. Adapter free reads were then processed with DADA2 (Callahan et al., 2016), following the DADA2 protocol (<https://benjjneb.github.io/dada2/tutorial.html>). For each pair of fastq files, we generated quality plots to guide fine-tuning of the data processing. Both forward and reverse read ends were trimmed to eliminate bases with a low-quality score, while maintaining enough overlap (20 bp) to allow the merging of forward and reverse reads. At this point, DADA2 utilizes the learned error rates in base calling to infer the number of error-free unique sequences in each sample (Callahan et al., 2016).

Dereplication and inference of sequence variants followed, then reads were merged and again quality checked while also removing chimeric reads with DADA2. Only amplicon sequence variants (ASVs) with more than 10 reads were considered for further analysis.

Taxonomy was assigned using the assignTaxonomy and assignSpecies functions from DADA2. assignTaxonomy is based on the naïve Bayesian classifier approach of Wang et al. (2007). Reads were taxonomically identified using the SILVA v.132 database (<https://www.arb-silva.de/>). The latter database was specifically chosen as it captures both prokaryotes and eukaryotes (including photosynthetic and nonphotosynthetic organisms) occurring in the ocean as well as in the sediments, to allow us to make a first assessment of which organisms' DNA is paleo-deposited and likely of ancient origin (expected to be detectable in both water and sediments). For the analysis of the bacterial community based on 16s rRNA sequencing, we removed reads that were classified as

chloroplast or mitochondria from each sample. The number of reads for each sample was normalized using the CSS normalization implemented in metagenomeSeq (Paulson et al., 2013).

2.8. *se*daDNA Extractions and Library Preparations

*se*daDNA extractions were undertaken at the specialized ancient DNA facilities of the Australian Centre for Ancient DNA (ACAD), The University of Adelaide, Australia. Before entering the lab, the outside of each sample bag was decontaminated by wiping with 3% bleach and exposing them to UV light for 5 min. *se*daDNA was extracted following either the “Si20_20 μ L” (KC06) or the “combined” (KC02, KC14) protocol described in L. Armbrrecht et al. (2020). Both techniques involve bead-beating to lyse cells at the initial step of *se*daDNA extraction, and DNA binding in silica-solution to retain small DNA fragments. In the “combined” technique, the bead-beating is preceded by an additional overnight sediment incubation step in ethylenediaminetetraacetic acid, which has been shown to increase the recovery of marine eukaryote *se*daDNA (Armbrrecht et al., 2020). KC06 *se*daDNA extractions were performed in 2017, before the “combined” protocol had been developed, however, due to the marked lithology (diatom-ooze/mats) of KC06, we deemed these samples an important addition to this study. To identify potential contaminant DNA, one to two extraction blank controls (EBCs), in which empty tubes were treated with the same extraction protocol as the samples (including sequencing), were run alongside each set of extractions of KC02, KC06, and KC14 samples (Table 1).

Metagenomic shotgun libraries were also prepared following Armbrrecht et al. (2020), with a description provided in Notes 2 in Supporting Information S1. This protocol includes the preparation of double-indexed libraries, where the libraries undergo a first amplification (with two unique 7 base-pair (bp) barcodes) using IS7/IS8 primers, and then a second amplification using IS4 and GAI Indexing Primers (Meyer & Kircher, 2010). In the first amplification, we used 13 amplification cycles for KC06 and 22 cycles for KC02 and KC14—the latter was adjusted based on protocol optimizations from Armbrrecht et al. (2020). In the second amplification, we used 13 cycles for all samples. The libraries were sequenced on Illumina platforms at the Australian Cancer Research Foundation Cancer Genomics Facility & Centre for Cancer Biology (ACRF), Adelaide (KC06: NextSeq 2 \times 150 bp), and the Garvan Institute for Medical Research, Sydney, Australia (KC02: NextSeq 2 \times 75 bp; KC14: HiSeq 2 \times 150 bp).

2.9. *se*daDNA Data Processing and Analysis

The sequencing data were processed and filtered as previously described (Armbrrecht, Eisenhofer, et al., 2021; Armbrrecht, Hallegraeff, et al., 2021; Armbrrecht et al., 2020). Data filtering involved the removal of sequences <25 bp (AdapterRemoval v. 2.1.7-foss-2016a; Schubert et al., 2016), and of low complexity (Komplexity software, E. L. Clarke et al., 2019) and duplicate reads (“dedupe” tool in BBMap v.37.36), and quality control after each step (FastQC v.0.11.4, Babraham Bioinformatics; MultiQC v.1.0.dev0; Ewels et al., 2016). To retain the maximum number of reads and largest possible diversity, the data set was processed without standardizing (i.e., nonrarefying, Cameron et al., 2021). We used the SILVA SSURef NR 132 database as a reference to build a MALT index, and sequences were aligned using MALT (version 0.4.0; semiglobal alignment; Herbig et al., 2016). The resulting .blastn files were converted to .rma6 files using the Blast2RMA tool in MEGAN (version 6_18_9; Huson et al., 2016). Subtractive filtering (i.e., subtracting reads for species identified in EBCs from samples) was conducted separately for each site’s data set (KC02, KC06, and KC14) in MEGAN CE (version 6.21.12).

The filtered read counts per taxon and site were exported for further downstream analysis ($n_{\text{KC02}} = 2$; $n_{\text{KC06}} = 7$, with read counts of the duplicate KC06 samples at 260 cm below sea floor [cmbsf] averaged; $n_{\text{KC14}} = 3$), while taxa determined in the extraction blanks are listed in Table S8 in Supporting Information S1. First, we exported all data at domain level for a first overview of prokaryote and eukaryote contribution and determined relative abundances. Next, we exported bacteria and eukaryote read counts at phylum level; this level was chosen as it provides adequate resolution of major eukaryote groups, for example, diatoms, retaria, chlorophytes, and for consistency with *se*daDNA bacteria data where several groups were not classified below phylum level (data exported on order level, where possible, are provided in Supporting Information S1). For Bacteria, the groups “Bacteria” and “environmental samples <bacteria, superkingdom Bacteria>” were grouped into one group named “Bacteria.” For Eukaryota, taxa that were identified as “incertae sedis” and “environmental sample” were grouped with the associated larger group (e.g., “fungi, incertae sedis” was grouped with “Fungi”; “environmental samples eukaryotes” was grouped with Eukaryota; and clade “Stramenopiles” was grouped with “Stramenopiles”). Few

Archaea reads were identified (see Section 3), and these data are provided with Notes 4, Figure S5, and Table S6 in Supporting Information S1.

2.10. Data Analysis and Visualization

Data analysis and visualization were performed within R statistical software (R Core Team, 2020) leveraging the *phyloseq* (McMurdie & Holmes, 2013), *vegan* (Oksanen et al., 2020), *tidyverse* (Wickham et al., 2019), and *pals* (Wright, 2021) packages. Alpha diversity for the 16 and 18S rRNA was calculated on rarefied data leveraging the *estimate_richness* script in *phyloseq*. A nonparametric Kruskal-Wallis test was then applied to test the significance of the difference in alpha diversity. Dissimilarity between samples in the water column was visualized on a multi-dimensional scaling plot based on a Bray-Curtis dissimilarity matrix of the bacterial and eukaryotic community, respectively, calculated within the *phyloseq* environment and plotted using *ggplot*.

Prior to constructing taxa plots, some taxa were grouped/renamed to allow for consistency and easier comparison between the taxa determined in the water column and sediment samples (see Table S4 in Supporting Information S1).

3. Results

3.1. Seawater Conditions and Variability

Different environmental conditions characterized the water column at the three sites. CTD05 and CTD16 had similar surface seawater temperatures ($\sim 1^{\circ}\text{C}$) declining sharply to -1.5°C at the chl max (Figure 2). The CTD03 profile has different characteristics, with the surface temperature (-0.2°C) and the salinity lower than in the two other sites, while just below the surface the temperature increased. CTD03 was collected in proximity to melting sea ice, which likely explains these differences. A sharp decline in temperature at the chl max is consistent with the other two sites (Figure 2). Below 1,000 m, the three sites had comparable physicochemical environmental conditions. Silicate and phosphate concentrations at all three sites were lower at the surface (average 57.8 and 1.94 μM , respectively) and then increased with depth (Table S1 in Supporting Information S1), whereas nitrite concentrations were higher at the surface and decreased with depth (Figure 2).

3.2. Sediment Lithology, Age, and Silica Content

The lower part of KC02 (240–100 cmbfs) consists of massive silty clays/clays, with the bottom of the core dating back to the last glacial at 21,809 ka BP at 230 cmbfs. Low numbers of foraminifers and dropstones were found throughout the core (Figure 3). The lower part of KC14 (345–120 cmbfs) dates back to the last glacial period at 22,823 ka BP (330 cmbfs) and consists of bioturbated clay-rich sediments with dropstones, with a distinct laminated interval from 255 to 235 cmbfs (Figure 3). Glacial sediments in KC02 and KC14 contain trace concentrations of biogenic silica ($<3\%$ on average) and low Si/Al ratios (average 14.3–14.9 for the bottom 100 cmbfs, respectively), which gradually transition to diatom-rich sediments in the Holocene (average biogenic silica 30% and 36%; average Si/Al ratios 26.9–33.5 for top 100 cmbfs, respectively). Biogenic silica concentrations initially start to increase from ~ 100 cmbfs in KC02 and ~ 150 cmbfs in KC14 after which the sediments are dominated by diatom ooze with silty clay, and a higher proportion of sand than observed in the fine clay-rich glacial sediments. In contrast, KC06 is composed primarily of diatom ooze and does not record a transition from glacial (mud-rich) to Holocene (silty diatom ooze) conditions revealed by the sediment composition at sites in the west. The lower section of KC06 (280–120 cmbfs) is characterized predominantly by diatom ooze (Figure 3), including the presence of diatom mats. The Si/Al ratios in the top 100 cmbfs of KC06 are comparable to the Holocene Si/Al ratios of the cores in the west but are much higher (average 70.5) in the bottom 100 cmbfs. The shipboard observations and magnetic susceptibility record (Figure 3) revealed that the upper section of KC06 contains a higher proportion of coarser terrigenous components composed of silty to sandy clay, compared to the Holocene sections of KC02 and KC14. The high Si/Al ratios observed in the bottom 100 cmbfs of KC06 during the period dominated by diatom mat deposition are likely related to low terrigenous inputs and hence low Al abundance. Overall KC06 records a switch in environmental conditions from those dominated by diatom mats to more typical Holocene-like deposition dominated by clay-rich diatom ooze, as seen at the western core sites.

3.3. Proportion of Reads Assigned to Bacteria and Eukaryota Using Modern DNA in the Water Column

We identified a total of 9,874 ASVs based on the 16S rRNA sequencing across the different samples. Of these, 6,025 belonged to Bacteria and the rest were assigned to either chloroplast or mitochondria sequences and were therefore removed from the data set. A total of 55% of the ASVs could be assigned up to genus level, while the remaining

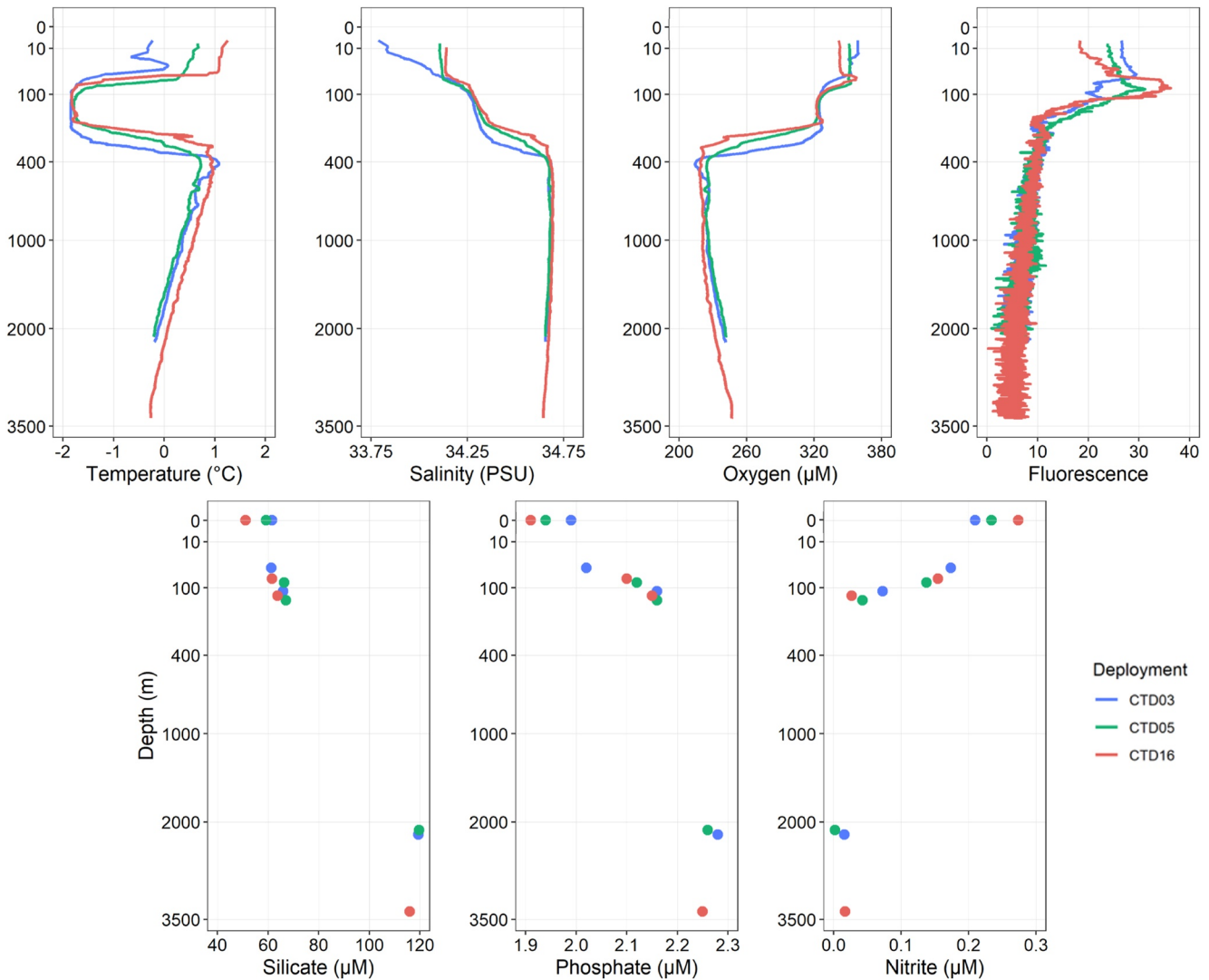


Figure 2. Physicochemical profiles of the water column. Note that the y-axis scale has been square root transformed to better visualize the top 100 m (where the bulk of the samples were taken). Temperature, salinity, oxygen, and fluorescence were derived from conductivity–temperature–depth (CTD) data while silicate, phosphate, and nitrite were derived from hydrochemistry data.

44% could only be classified up to family level. For the eukaryote community, a total of 6,732 ASVs were retrieved based on the sequencing of the 18S rRNA. At the class level, 21% of the identified ASVs could not be identified, and at genus level, just 32% of the total ASVs could be classified. We observed a trend toward decreasing numbers of reads with depth, which was particularly noticeable for diatoms (regression coefficient $r = -0.74$, $p = 0.0074$).

3.4. Proportion of Reads Assigned to Bacteria and Eukaryota Using *sedDNA*

We retrieved a total of 9,016 assigned reads across all KC samples, which included 7,988 reads assigned to Bacteria, 264 to Archaea, and 800 reads assigned to Eukaryota (Figure S1 in Supporting Information S1). In relative abundances, Bacteria were the most represented domain (87% on average across all samples, followed by Eukaryota (9%), Archaea (3%), and “cellular organisms” (2%; Figure S1 in Supporting Information S1). In sample KC06 170 cmbfs, we identified ~60% Bacteria and ~40% Eukaryota, however, very few reads (32) were retrieved for this sample. No Archaea were identified in three samples at site KC06 (0, 66, and 170 cmbfs; Figure S1 in Supporting Information S1). We did not observe any trend in the number of reads recovered from younger to older samples as with the water column modern DNA data, however, this might be due to the relatively limited number of *sedDNA* samples per site (≤ 6 samples).

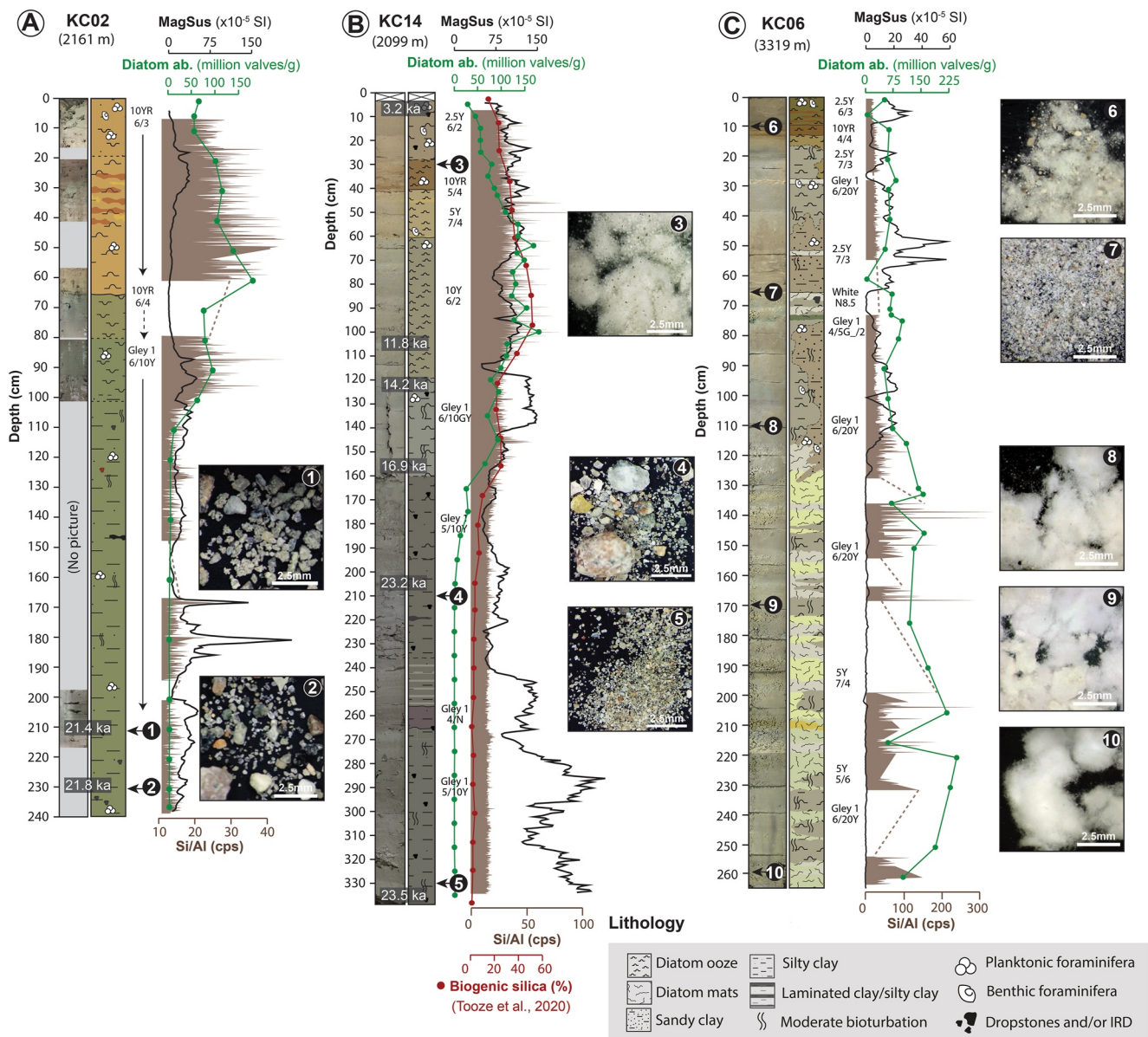


Figure 3. Kastan Core lithology. Lithology of Kastan Cores KC02, KC14, and KC06 and photos of the coarse fraction (>63 μm) at the same/similar depths (cmbsf) to where *seadaDNA* samples were taken. For details on magnetic susceptibility (MagSus), Si/Al ratios from scanning X-ray fluorescence, KC02 ages, and diatom abundance data, see Tables S2–S3 in Supporting Information S1. Figure adapted and modified based on Figure 49 and Appendix 5 of Armand et al. (2018).

We identified both prokaryotes and eukaryotes in the EBCs that were processed alongside *seadaDNA* samples from each core. The number of reads per identified contaminant taxon was mostly low (<10 reads per taxon per sample), however, the two eukaryote taxa Chromadorea and Thecofilosea were identified with a higher number of reads (22 and 18, respectively [in one EBC each]). In the KC02 and KC14 EBCs, we identified few contaminant taxa, but both included *Pseudomonas* and Thecofilosea. The taxa composition in the KC06 EBCs was slightly different to KC02 and KC14, in that more and primarily prokaryote taxa were identified (Table S8 in Supporting Information S1).

3.5. Bacteria in the Water Column (Modern DNA, Phylum Level)

Proteobacteria dominated in relative abundance at each site, followed by Bacteroidetes, Actinobacteria, and Planctomycetes. The relative abundance of Proteobacteria was >75% at each site for surface samples, followed by Bacteroidetes ~20% at each site. While the Proteobacteria and Bacteroidetes decreased in relative abundance

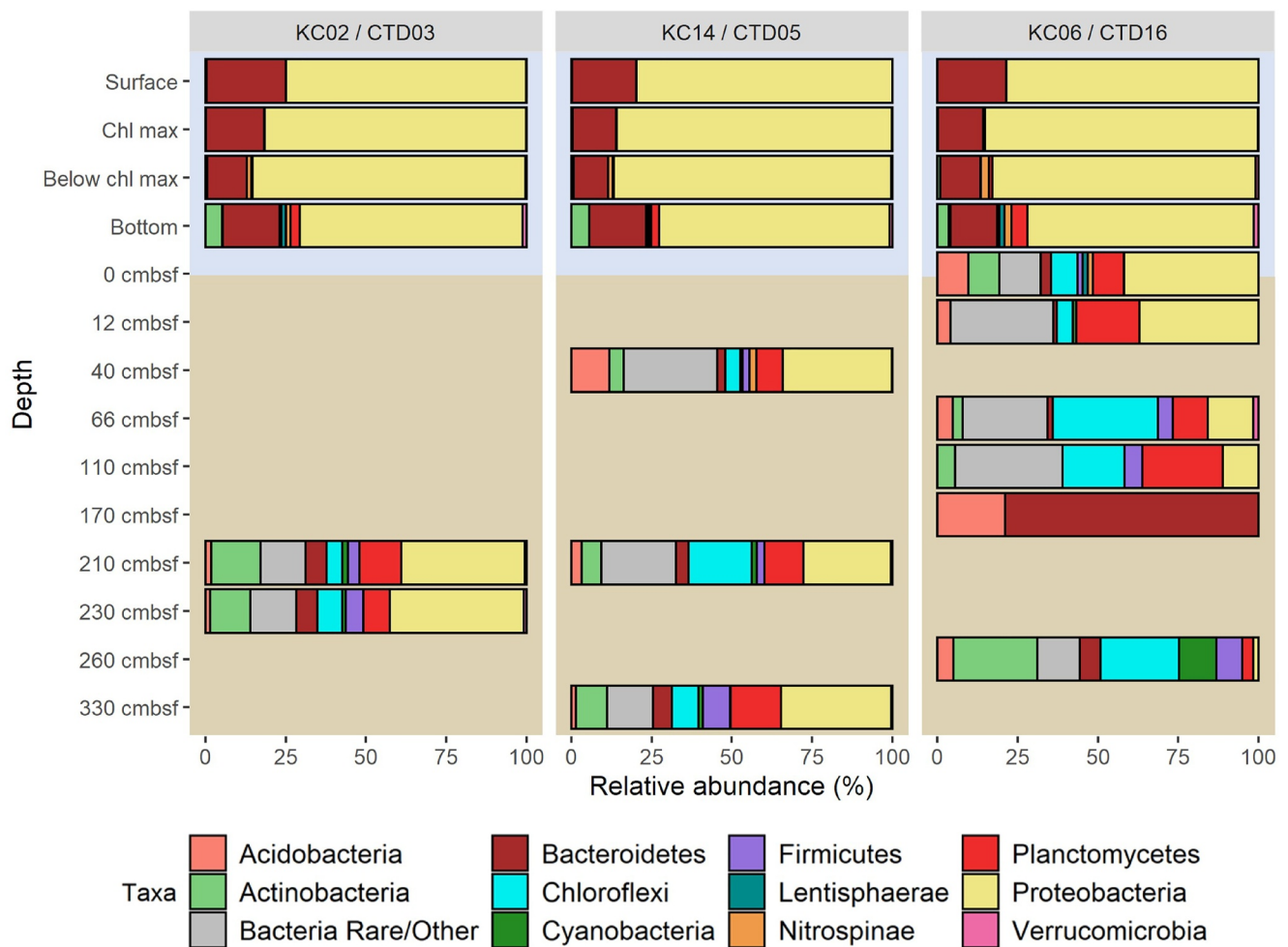


Figure 4. Relative abundance of Bacteria identified in the Sabrina Coast water column and sediments. Relative abundance of the water column bacteria (modern DNA) was derived from 16S rRNA amplicon sequencing (light blue background). Relative abundance of sediment bacteria (*sead*DNA) was derived from shotgun sequencing (light brown background). Taxonomic information was extracted at the phylum level, and visualized are taxa with a relative abundance >1% in at least one sample. Sample KC06 260 cbsf displays the average of the duplicate samples at this depth, and note that KC06 read numbers are low (309 reads total). The legend reads from top to bottom, then from left to right. For read count data, see publicly available data (Armbrecht & Focardi, 2022, modern DNA) and Table S5 in Supporting Information S1 (*sead*DNA). Cbsf, centimeters below seafloor.

with water depth, Actinobacteria increased by, on average, 42-fold from the surface to the deepest samples at all sites, going from ~0.05% to ~5% relative abundance at CTD03 and CTD05, and ~3% relative abundance at CTD16 (Figure 4). Both Nitrospinae and Planctomycetes were absent in the surface waters, but their relative abundance increased in the bottom water samples. Planctomycetes specifically contributed up to ~2.5% relative abundance of the bacterial community in the bottom waters at CTD03 and CTD05, and 5% relative abundance at CTD16. Investigation into diversity patterns showed an overall significant increase in Shannon diversity with depth ($p < 0.05$; Notes 3 and Figure S3 in Supporting Information S1). A multidimensional scaling plot analysis at the ASV level revealed that the samples clustered tightly with depth, and more specifically by euphotic zone and aphotic zones, with the first axis of the plot explaining 64% of the dissimilarity (Figure S4 in Supporting Information S1).

3.6. Bacteria in the Sediments (*sead*DNA, Phylum Level)

KC02 and KC14 bacterial taxonomic depth profiles were very similar to each other, while those at KC06 differed slightly (Figure 4). Bacteria (not further classified; all samples except KC06 170 cbsf), Bacteroidetes (especially sample KC06 170 cbsf), Proteobacteria (especially at KC02 and KC14), and Planctomycetes and

Chloroflexi (both at all sites) were particularly abundant. Bacteria that only occurred at KC02 and KC14 (but not KC06) included the Candidatus taxa, the Patescibacteria and Microgenomates groups, Fibrobacteres, Fusobacteria, Nitrospirae, PVC group, Chlamydiae, Kiritimatiellaeota, Armatimonadetes, and Tenericutes (Figure 4). Bacteria that only occurred at KC06 included Nitrospirae. One sample (KC06 170 cmbsf) differed from all other samples in that only Acidobacteria and Bacteroidetes were identified (Figure 4).

There were 16 bacterial phyla that are common to the water column and sediments: Acidobacteria, Bacteroidetes, Fibrobacteres, Fusobacteria, Nitrospirae, Nitrospirae, Proteobacteria, Lentisphaerae, Planctomycetes, Verrucomicrobia, Actinobacteria, Armatimonadetes, Chloroflexi, Cyanobacteria, Firmicutes, and Tenericutes. Eleven of these are visualized in Figure 4 (Bacteria), as five were rare (i.e., did not occur with at least 1% relative abundance in any sample: Fibrobacteres, Fusobacteria, Nitrospirae, Armatimonadetes, and Tenericutes).

3.7. Eukaryota in the Water Column (Modern DNA)

Eukaryota showed a much higher diversity at the phylum level compared to bacteria, with 24 phyla identified across the three sites. Ochrophyta/diatoms dominated the surface eukaryotic community at CTD03 and CTD05 (Figure 5), with a relative abundance of 55% and 44%, respectively, followed by Haptophyta (12.5% at CTD03, 14% at CTD05) and Dinoflagellata (3.5% at CTD03, 14.9% at CTD05). For CTD16, the Ochrophyta/diatoms and Dinoflagellata have comparable relative abundance (30% and 32%, respectively) followed by Haptophyta (8.8%). At the chl max, the eukaryotic composition was similar at the three sites, with Ochrophyta and Dinoflagellata being the most abundant phyla at all three sites, followed by Haptophyta, Chlorophyta, and Ciliophora. For the bottom depth samples, the eukaryotic composition was similar at CTD03 and CTD05 but different for CTD16. CTD03 and CTD05 had a similar relative abundance of Retaria, Alveolata, and Dinoflagellata, and both sites had a low Ochrophyta/diatom signature (relative abundances of 5% at CTD03, 12% at CTD05), while Cnidaria were only detected at CTD3. At CTD16, Cnidaria were highly abundant (83%), followed by Retaria and Alveolata, while an Ochrophyta/diatom signature was absent from this site. For exact read count data, see publicly available data (Armbrecht & Focardi, 2022).

3.8. Eukaryota in the Sediments (*seadDNA*)

A total of 42 eukaryote phyla across all samples and sites were identified in the *seadDNA* data (from 792 reads in total; Figure 5 and Table S7 in Supporting Information S1). The most abundant phylum was Retaria (Figure 5) and more specifically the class Polycystinea (284 reads in total), which were well represented at KC02 (~40% of Eukaryota at both depths) and at KC14 (~50% and ~15% of Eukaryota at 210 and 330 cmbsf; Table S7 in Supporting Information S1). Other major eukaryotic plankton groups, such as Haptista (including the coccolithophores), Dinophyceae, Foraminifera, and Bacillariophyta (diatoms), were detected in relatively low abundance (<10% of Eukaryota; Figure 5 and Table S7 in Supporting Information S1). As with the signals found for Bacteria, the Eukaryota composition was relatively similar at KC02 and KC14, but differed at KC06. Only seven taxonomic groups were identified at KC06 (Eukaryota, Ascomycota, Basidiomycota, Bilateria, Chordata, Bacillariophyta, and Streptophyta, <2 reads per sample; except Ascomycota with 12 reads at KC06 170 cmbsf), and there were no reads in the two upper-most samples (Figure 5). Read counts per taxon per sample are provided in Table S7 in Supporting Information S1.

There were 11 eukaryote taxa that are common to the water column and sediments: Arthropoda, Ascomycota, Basidiomycota, Bryozoa, Cercozoa, Ciliophora, Cnidaria, Ctenophora, Ochrophyta/Bacillariophyta, Haptista, and Retaria.

4. Discussion

Polar environments are important study regions in the context of ongoing climate change, and so are the responses of marine microbial communities due to their function as major drivers of the global carbon cycles (Arrigo et al., 2008). Despite the increasing number of genomic-based studies conducted around Antarctica (e.g., M. S. Brown et al., 2021; Gionfriddo et al., 2016; Lin et al., 2021), knowledge of the taxonomic diversity of Antarctic microbial communities and their distribution throughout the water column, as well as postmortem DNA preservation in the underlying sediments, is still in its infancy. In the following, we discuss our findings on the

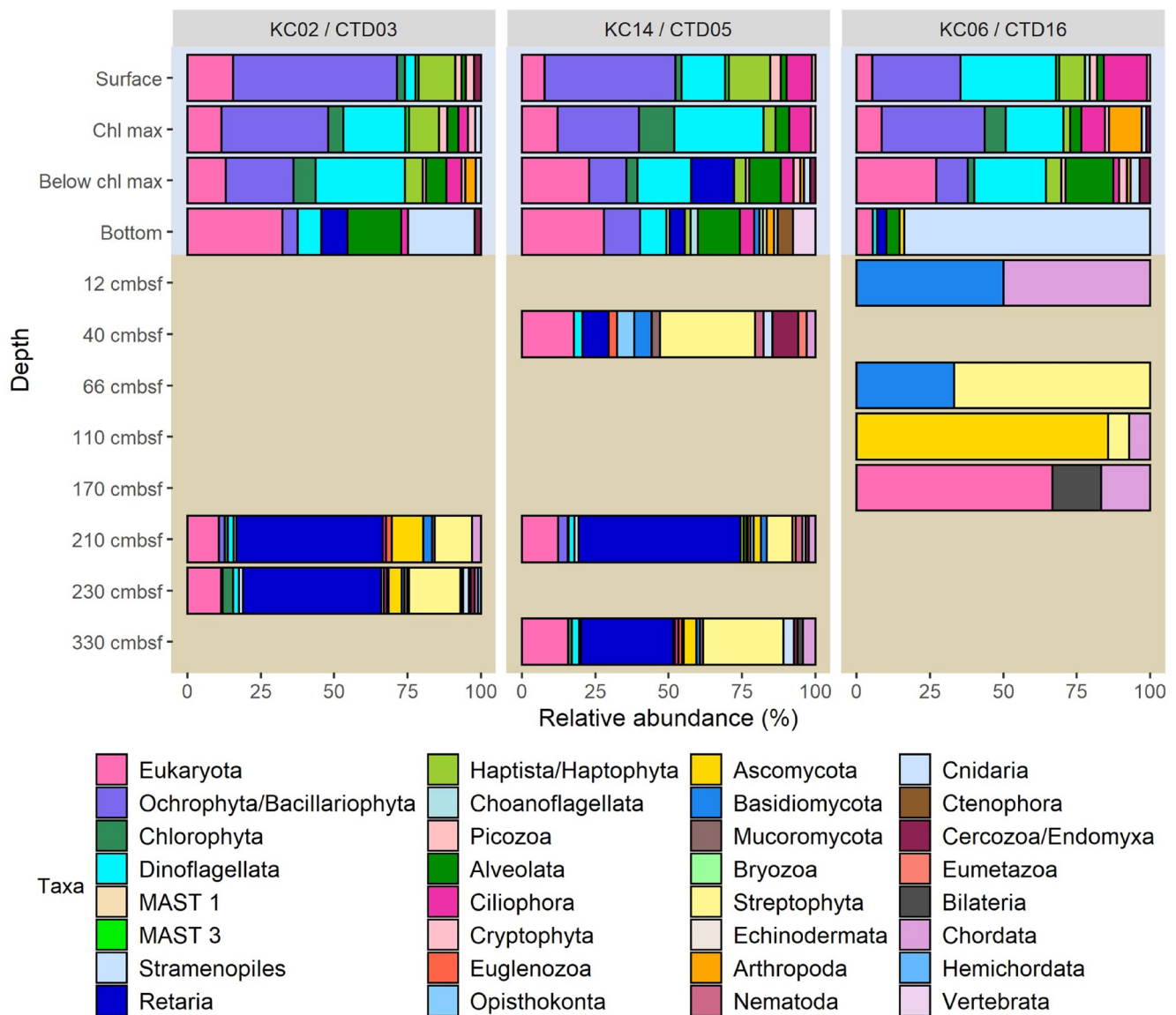


Figure 5. Relative abundance of Eukaryota identified in the Sabrina Coast water column and sediments. Relative abundance of the water column eukaryotes (modern DNA) was derived from 18S rRNA amplicon sequencing (light blue background). Relative abundance of sediment eukaryotes (*seDa*DNA) was derived from shotgun sequencing (light brown background). Taxonomic information was extracted at the phylum level, and visualized are taxa with a relative abundance >1% in at least one sample. Sample KC06 260 cmbsf displays the average of the duplicate samples at this depth, and note that *seDa*DNA data of KC06 are based on very low read numbers (22 reads total). The legend reads from top to bottom, then from left to right. For count data, see publicly available data (Armbrecht & Focardi, 2022, modern DNA) and Table S7 in Supporting Information S1 (*seDa*DNA). Cmbsf, centimeters below seafloor.

DNA-derived prokaryote and eukaryote composition of both the modern ocean and the underlying sediments in the climatically important Sabrina Coast region, East Antarctica.

4.1. Water Column Bacteria

Bacterial communities in the water column were distinctly dominated by Proteobacteria (~70%). This finding is not surprising, given their reported high abundance in all oceans, including polar oceans and in surface as well as deep waters (Z. Zhou et al., 2020). Within the Proteobacteria, members of the SAR11 clade were dominant in each sample, comprising roughly 50% of the surface communities and declining to ~13% of the bottom water bacterial communities. Members of the SAR11 clade represent the most abundant heterotrophic bacteria in the global ocean (M. V. Brown et al., 2012; Delmont et al., 2019; Giovannoni, 2017; Morris et al., 2002). Due to

the temperature being linked to ecotype partitioning, SAR11 has been proposed as a potential marker species to assess the influx of tropical ecotypes toward the polar region (M. V. Brown et al., 2012; Delmont et al., 2019). Here, the cold water adapted SAR11 clade Ia, which is known to be prominent in the Southern Ocean (M. V. Brown et al., 2012; Delmont et al., 2019), was the most abundant within the SAR11 clade. SAR11 occurred at a lower relative abundance at site CTD03 (46%) compared to the other surface sites (>50%). CTD03 was located in the proximity of an iceberg and was strongly influenced by the presence of ice-melting water, resulting in a lower surface temperature. Ice-melting has also been linked to the release of trace nutrients such as iron (Raiswell et al., 2016) that are considered limiting factors for phytoplankton growth and could potentially favor an increase in primary producers and their associated microbiome. Accordingly, this site was also characterized by high proportions of members of the Flavobacteriales order. Members of the Flavobacteriales (Bacteroidetes) are known to be abundant in the Southern Ocean and especially in euphotic Antarctic water (Wilkins et al., 2013), where they play a crucial role in the utilization and remineralization of organic matter produced by phytoplankton (Williams et al., 2013). Hence, they are usually found in association with marine primary producers such as diatoms. Phycisphaerales and Pirurellales (Planctomycetes) are often found in marine anoxic and subsurface marine sediment (Inagaki et al., 2006), even though when cultivated they are known to be facultative aerobes. Some studies have indicated the possibility that these taxa are able to degrade organic matter derived from algae (Cho et al., 2020; Morris et al., 2006) and have hypothesized their ecological role in the remineralization of recalcitrant organic matter of *Phaeocystis* origins in the benthic ecosystem.

4.2. Sediment Bacteria

Disentangling ancient (i.e., stemming from dead, and/or paleo-deposited organisms) from actively living DNA signals in sediments is a matter of high priority in the paleo-genomics research field and is critical for improving the accuracy of paleo-environmental reconstructions (Capo et al., 2022). In this context, bacteria are a particularly challenging group of organisms, since they can survive under extreme conditions, including in deep seafloor sediments down to 2.5 km (Imachi et al., 2019; Inagaki et al., 2015).

A total of 11 abundant and 5 rare bacterial phyla that were detected in the water column were also detected in the sediments. As with the water column, Proteobacteria were the dominant bacterial phylum in the sediments (~25% on average across all samples) and occurred in all samples except KC06 170 cmbsf. This result is consistent with previous studies on Southern Ocean and Antarctic sediments, which found Proteobacteria to be relatively abundant in sediments (Cho et al., 2020; Learman et al., 2016). Therefore, Proteobacteria seem to be able to survive in both ocean and sediment environments, with the DNA detected in the sediment record possibly being a mix of modern and ancient Proteobacteria DNA. Proteobacteria are often found in diatom-dominated waters (Cho et al., 2020; Learman et al., 2016), which may be useful for *sedDNA* studies in which diatom *sedDNA* is difficult to extract, as the Proteobacteria signals may be indirectly reflecting past diatom presence. However, more research is required to confirm whether the apparent co-occurrence of proteobacteria (or specific proteobacteria orders) could be used as a proxy of primary producers' presence in surface waters and whether these eukaryote-bacteria associations could be explored as paleo-composition indicators. A similar example is comprised by Planctomycetes-*Phaeocystis* associations in surface waters (Cho et al., 2020).

Bacteroidetes and Actinobacteria were also detected in water and sediments, and as for Proteobacteria, have previously been reported to live in Antarctic sediments (M. Y. Zhou et al., 2013). Therefore, the DNA from Bacteroidetes and Actinobacteria in the sediments might also be a mix of modern and ancient DNA, although these two phyla were only identified in KC06 170 cmbsf, alongside no other bacteria. The latter might be due to different environmental conditions prevailing at the time of paleo-deposition and could indicate that these sediments are indeed from a very different time period (in particular, MIS5, which includes MIS5e, a major interglacial period; Rohling et al., 2008), however, this is speculative due to uncertainty in the KC06 age model and possible biases of the KC06 *sedDNA* extraction protocol (see Section 4.5).

It is noticeable that the other 13 bacterial phyla that were present in the water column, but at lower relative abundance, had a more pronounced relative abundance in the sediments (Fibrobacteres, Fusobacteria, Nitrospinae, Nitrospirae, Lentisphaerae, Planctomycetes, Verrucomicrobia, Actinobacteria, Armatimonadetes, Chloroflexi, Cyanobacteria, Firmicutes, and Tenericutes). It is likely that this pattern is due to the overall much lower yield of ancient compared to modern DNA, which, combined with potential differential preservation of the DNA of individual species, may have led to the relative abundances being skewed toward the presence of these organisms.

Additionally, nuclease activity in the upper sediment layers might impact the long-term preservation of *seadDNA* (Zimmermann et al., 2021). To shed light on these important DNA preservation-related questions, future studies could investigate modern and *seadDNA* on a quantitative scale, which unfortunately, due to the differences in the approaches to analysis of modern and ancient DNA in this study, was not possible here.

4.3. Water Column Eukaryota

Diatoms (Ochrophyta) dominated from the surface waters down to the chl max depth at all sites, with CTD03 having the highest abundance of diatoms in the surface waters. The latter might be due to slightly higher nutrient concentrations (silicate and phosphate), and a potential higher iron concentration due to being in the vicinity of melting-ice (Raiswell et al., 2016; see Section 4.1). Below the chl max, the relative diatom abundances decreased considerably. The latter could be a consequence of dissolution, considering that both relative and non-normalized abundance of diatom reads decreased with increasing water depth, but also could be due to “dilution” of diatom reads with DNA from other organisms, or a combination of both factors. Silicate concentrations increase with depth, which further suggests that diatom-dissolution might play a role in this process (less frustules, more silicate at deeper water depths). Dinoflagellates followed a very similar pattern to diatoms, being relatively abundant in the surface waters, but less so in deep waters. The same pattern was observed for Haptophytes. These findings suggest that much of the DNA that is representative of surface water column phytoplankton at these Southern Ocean sites degrades and/or is being consumed while sinking, more so than being degraded after burial.

In a contrary pattern, Retaria were found mostly below the chl max and in deep waters. Retaria include the unicellular predatory Foraminifera and Radiolaria, they are globally distributed and are highly abundant in the Southern Ocean south of 45°S, with several classes adapted to thrive from the surface to the deep Ocean (Abelmann & Gowing, 1997; Biard, 2022; Boltovskoy, 2017). Retaria play a key role in the carbon export in the global Ocean (Guidi et al., 2016) with classes belonging to this phylum often found in sediment traps (Fontanez et al., 2015). This might indicate that Radiolaria and/or Foraminifera DNA is transported to deeper depths than other taxa and subsequently has a higher chance of becoming preserved in seafloor sediments.

4.4. Sediment Eukaryota

The eukaryote composition in the sediments was quite different from the water column composition at all sites. Little diatom, dinoflagellate, and haptophyte *seadDNA* was detected, thus, considering the strong decrease of modern DNA of these phytoplankton groups with increasing water depth, it seems likely that very little of their DNA reaches the seafloor to become preserved in sediments in the Sabrina Coast region. The few diatom sequences detected in *seadDNA* (13 in total) were assigned at a relatively high taxonomic level, that is, Bacillariophyta, *Mediophyceae* (which include the genus *Chaetoceros*), while two reads were identified at slightly higher taxonomic resolution (*Proboscia*, 1 read, and Biddulphiophycidae, 1 read; both in KC14 210 cmbfs). Microscopy data from the same samples, however, showed a high relative abundance of *Fragilariopsis kerguelensis* in all three cores, and, to a lesser degree, *Rhizosolenia* spp. and *Chaetoceros* subg. *Hyalochaete*, amongst a few other, rarer species (Table S3 in Supporting Information S1). Therefore, there appears to be a disconnect in our study area between diatom frustules and diatom DNA sinking through the water column to the seafloor and becoming preserved there. Diatom DNA seems to degrade while sinking, and it is possible that traces of intact *seadDNA* might be linked to diatom DNA and frustules being exported via fecal pellets, in which they are more protected from dissolution and remineralization.

Polycystinea were the most abundant eukaryote group detected by *seadDNA*, especially at depths below 210 cmbfs at KC02 and KC14. Polycystinea are a group of Radiolarians, and as water column data showed, their DNA contributes a relatively high proportion to the bottom water communities, which, due to the proximity to the seafloor, might promote their good preservation in the underlying sediments. It appears obvious that degradation of DNA with increasing water depth is a major driver of what DNA becomes preserved in the sediments (especially, for surface-dwelling organisms in a deep water column) and ultimately will impact on the paleo-environmental reconstructions. Here, the dominant radiolarian group detected were Collodaria, especially *Collophidium*, which do not have siliceous skeletons, explaining why they are not observed in the fossil record (Ishitani et al., 2012). Previously, Pernice et al. (2016) determined Collodaria as a dominant group in the deep ocean (using water samples from the Atlantic, Pacific, and Indian Ocean collected between 3,000 and

4,000 m depth), again, reinforcing that proximity of water column organisms to the seafloor plays a role in their representation in the *seda*DNA record. Collodaria are colonial, and radiolarian colonies have been shown to have exceptionally high SSU gene copy numbers ($37,474 \pm 17,799$ per colonial cell; Biard, 2022) compared to a few hundred in diatoms (Godhe et al., 2008), which may bias SSU-based abundance data toward colonial radiolaria. Collodaria nourish through photosynthetic endosymbionts, which provides a conundrum as these would not be able to survive in the ice-covered environment experienced during the last glacial maximum at our sites on the Sabrina Coast (when Collodaria reads were found). It is possible that the Collodaria reads were misassigned, which we tested by reblasting against the NCBI database, providing best hits for “uncultured marine eukaryotes” (i.e., the true identity of our sequences is not [yet] known), as well as for Collodaria (i.e., an identity that is very similar to this group). It is also possible that we detected a trace amount of Collodaria from the previous interglacial signal in the glacial sediments, which had above-zero biogenic silica concentrations, coinciding with extinct and robust diatom species (Holder et al., 2020; Leventer, 2022; Table S3 in Supporting Information S1). Unfortunately, we only have one interglacial sample for comparison (KC14; 40 cmbsf), and clearly, more research is required over multiple glacial–interglacial cycles to determine abundance patterns of Collodaria through time. A final hypothesis is that these might be unknown deep-sea Collodaria populations whose ecology is different from surface collodarians (Pernice et al., 2016).

Basidiomycota and Ascomycota were detected, especially at KC06, and also occurred in the water column, suggesting they may survive in both environments. Careful interpretation is required, however, as especially fungi have been linked to contamination in *seda*DNA from deep seafloor archive samples stored over many years prior to analyses (Selway et al., 2022), although our samples were freshly collected, thus the latter possibility seems unlikely.

4.5. Limitations of the Study

KC02 and KC14 were collected at a water depth of $\sim 2,100$ m at the crest of ridges adjacent to underwater canyons, while KC06 was collected $\sim 1,200$ m deeper on the floor of a canyon (at 3,320 m water depth). Radiocarbon dates combined with lithological observations and diatom abundance data indicate that while KC02 and KC14 had the characteristic clay-rich last glacial maximum and deglacial sediments, and Holocene diatom oozes, KC06 was composed primarily of diatom ooze throughout the entire core (Armand et al., 2018). Due to this difference in sedimentology, we expected a high diatom *seda*DNA yield at site KC06. However, this was not the case, and in fact nearly no diatom *seda*DNA was recovered here (1 read). KC06 *seda*DNA was extracted prior to *seda*DNA extraction optimization protocols being established that maximize eukaryote *seda*DNA yield and diversity (Armbrecht et al., 2020). It is likely that suboptimal extraction techniques, and a lower cycle number in the first library amplification, may have influenced the very limited *seda*DNA yield for KC06 samples, especially for eukaryotes (total of 22 eukaryote reads). The optimized technique applied to KC02 and KC14 differs from the older protocol in that sediment samples are first incubated in ethylenediaminetetraacetic acid prior to mechanical extraction of DNA by bead-beating, which has been shown to increase the yield of extracellular, eukaryote DNA in sediments (Slon et al., 2017). However, bacterial *seda*DNA is also well resolved when using this new protocol (Armbrecht et al., 2020). As both eukaryote and prokaryote *seda*DNA yield was low in KC06, likely due to the above-mentioned protocol bias, the limited *seda*DNA data from KC06 should be interpreted with caution. More research on this core (or similarly diatom-rich sediment cores) is required to determine whether new, more optimized extraction protocols can increase *seda*DNA yield from diatom-rich cores, or whether the high silica content of the sediments could play a role in inhibiting *seda*DNA extraction efficiency (due to the high binding-capacity of silica, as has been suggested previously, Armbrecht, 2020).

5. Conclusions and Future Outlook

We report the first bacterial and eukaryote taxonomic profiles from surface water to deep ocean to sediments in the Totten Glacier region of Antarctica. Our results show that the genetic signals change considerably from surface to deep waters and into the sediments, with only fractions of major planktonic groups that thrive in surface waters still being detectable in bottom waters and sediments (e.g., diatoms), while others that are well represented in deeper waters appear to have a higher likelihood of becoming preserved in the sediments (e.g., radiolarians, in particular, collodaria). We suspect two explanations for these patterns, including (a) dissolution and degradation of DNA through the water column, so that little DNA arrives at the seafloor, and (b) different

SSU gene copy numbers per cell, where organisms that have higher copy numbers per cell are more likely to be detected in samples characterized by low biomass (e.g., radiolarians over diatoms in deep waters and sediments).

We suggest the following research avenues to provide more clarity on these points in the future: (a) undertake a high-resolution study of the genetic signals detectable across the water–sediment interface to investigate change points in taxonomic profiles with depth; (b) analyze the entire genetic makeup of the bacterial and eukaryote communities, for example, by using a larger database (such as the NCBI database) rather than only one gene (here, the SSU database), which might help to retrieve better taxonomic signatures that are less well represented in the SSU database; (c) explore co-occurrence and symbiotic relationships of prokaryotes and eukaryotes in further detail to identify whether certain prokaryote taxa could be used as proxies for eukaryote DNA that are rare, and/or difficult to detect or extract. While overall trends in current and past composition can be inferred from modern and *sed*aDNA, these fine-scale biases and interactions will be important to consider and improve in future studies, especially when using *sed*aDNA as a proxy for paleo-environmental reconstructions.

Conflict of Interest

The authors declare no conflicts of interest relevant to this study.

Data Availability Statement

The physical and chemical oceanographic data used in this study are publicly available at the CSIRO Ocean and Atmosphere data trawler repository (https://www.cmar.csiro.au/data/trawler/survey_details.cfm?survey=IN2017_V01). The diatom data are archived at: Quantitative Diatom data collected from the 2017 *RV Investigator* voyage, *Australian Antarctic Data Centre*—doi:10.26179/Scad45a7cb140 (Leventer, 2022). The genetic data used in this study are available at the University of Tasmania Data Portal (<https://dx.doi.org/10.25959/4pd2-b503>, Armbrecht & Focardi, 2022). The *sed*aDNA data can be opened in the free software MEGAN CE (Huson et al., 2016) to view the associated taxonomy and raw read counts per sample. The modern DNA ASV sequence data are provided in form of a table (one for bacteria, one for eukaryotes) and also contain taxonomy and raw count for each sample.

Acknowledgments

We thank the Marine National Facility, the IN2017_V01 scientific party led by the Chief Scientists L. K. Armand and P. O'Brien, MNF support staff, and ASP crew members led by Capt. M. Watson for their help and support onboard the *RV Investigator*. This project was supported through funding from the Australian Government's Australian Antarctic Science Grant Programs (AAS 4333 and AAS 4419) and the Australian Research Council's Discovery Projects funding scheme (DP170100557). We thank the team at the Australian Centre for Ancient DNA (ACAD), The University of Adelaide, especially Corinne Preuss and Steve Johnson for their technical help during the *sed*aDNA laboratory work. LA was funded by an Australian Research Council Discovery Early Career Researcher Award (ARC DECRA DE210100929). The modern molecular data analysis was supported by an ARC Grant awarded to IP (FL140100021). KAL is supported by an Australian Research Training Program (RTP) scholarship. We acknowledge the use of imagery from the NASA Worldview application (<https://worldview.earthdata.nasa.gov>), part of the NASA Earth Observing System Data and Information System (EOSDIS). Open access publishing facilitated by University of Tasmania, as part of the Wiley - University of Tasmania agreement via the Council of Australian University Librarians.

References

- Abelmann, A., & Gowing, M. M. (1997). Spatial distribution pattern of living polycystine radiolarian taxa—Baseline study for paleoenvironmental reconstructions in the Southern Ocean (Atlantic sector). *Marine Micropaleontology*, 30(1–3), 3–28. [https://doi.org/10.1016/s0377-8398\(96\)00021-7](https://doi.org/10.1016/s0377-8398(96)00021-7)
- Armand, L. K., & O'Brien, P. E., & On-Board Scientific Party. (2018). *Interactions of the Totten Glacier with the Southern Ocean through multiple glacial cycles (IN2017-V01): Post-survey report*. Research School of Earth Sciences, Australian National University. <https://doi.org/10.4225/13/5acea64c48693>
- Armbrecht, L., Eisenhofer, R., Utge, J., Sibert, E. C., Rocha, F., Ward, R., et al. (2021). Paleo-diatom composition from Santa Barbara basin deep-sea sediments: A comparison of *18S-V9* and *diat-rbcL* metabarcoding vs shotgun metagenomics. *ISME Communications*, 1(1), 66. <https://doi.org/10.1038/s43705-021-00070-8>
- Armbrecht, L., & Focardi, A. (2022). Totten Glacier ocean & sediment DNA (IN2017_V01) [Dataset]. University of Tasmania Research Data Portal. <https://dx.doi.org/10.25959/4pd2-b503>
- Armbrecht, L., Hallegraeff, G., Bolch, C. J. S., Woodward, C., & Cooper, A. (2021). Hybridisation capture allows DNA damage analysis of ancient marine eukaryotes. *Scientific Reports*, 11(1), 3220. <https://doi.org/10.1038/s41598-021-82578-6>
- Armbrecht, L., Herrando-Pérez, S., Eisenhofer, R., Hallegraeff, G. M., Bolch, C. J., & Cooper, A. (2020). An optimized method for the extraction of ancient eukaryote DNA from marine sediments. *Molecular Ecology Resources*, 20(4), 906–919. <https://doi.org/10.1111/1755-0998.13162>
- Armbrecht, L., Weber, M. E., Raymo, M. E., Peck, V. L., Williams, T., Warnock, J., et al. (2022). Ancient marine sediment DNA reveals diatom transition in Antarctica. *Nature Communications*, 13(1), 5787. <https://doi.org/10.1038/s41467-022-33494-4>
- Armbrecht, L. (2020). The potential of sedimentary ancient DNA to reconstruct past ocean ecosystems. *Oceanography*, 33(2), 116–123. <https://doi.org/10.5670/oceanog.2020.211>
- Armbrecht, L., Coolen, M. J., Lejzerowicz, F., George, S. C., Negandhi, K., Suzuki, Y., et al. (2019). Ancient DNA from marine sediments: Precautions and considerations for seafloor coring, sample handling and data generation. *Earth-Science Reviews*, 196, 102887. <https://doi.org/10.1016/j.earscirev.2019.102887>
- Arrigo, K. R., van Dijken, G., & Long, M. (2008). Coastal Southern Ocean: A strong anthropogenic CO₂ sink. *Geophysical Research Letters*, 35, L21602. <https://doi.org/10.1029/2008GL035624>
- Barrenechea Angeles, I., Lejzerowicz, F., Cordier, T., Scheplitz, J., Kucera, M., Ariztegui, D., et al. (2020). Planktonic foraminifera eDNA signature deposited on the seafloor remains preserved after burial in marine sediments. *Scientific Reports*, 10(1), 20351. <https://doi.org/10.1038/s41598-020-77179-8>
- Bensi, M., Kovačević, V., Donda, F., O'Brien, P. E., Armbrecht, L., & Armand, L. (2022). Water masses distribution offshore the Sabrina Coast (East Antarctica). *Earth System Science Data*, 14(1), 65–78. <https://doi.org/10.5194/essd-14-65-2022>
- Biard, T. (2022). Diversity and ecology of Radiolaria in modern oceans. *Environmental Microbiology*, 24(5), 2179–2200. <https://doi.org/10.1111/1462-2920.16004>

- Boltovskoy, D. (2017). Vertical distribution patterns of Radiolaria Polycystina (Protista) in the World Ocean: Living ranges, isothermal submer-
sion and settling shells. *Journal of Plankton Research*, 39(2), 330–349. <https://doi.org/10.1093/plankt/fbx003>
- Brown, M. S., Bowman, J. S., Lin, Y., Feehan, C. J., Moreno, C. M., Cassar, N., et al. (2021). Low diversity of a key phytoplankton group along
the West Antarctic Peninsula. *Limnology & Oceanography*, 66(6), 2470–2480. <https://doi.org/10.1002/lno.11765>
- Brown, M. V., Lauro, F. M., Demaere, M. Z., Muir, L., Wilkins, D., Thomas, T., et al. (2012). Global biogeography of SAR11 marine bacteria.
Molecular Systems Biology, 8(1), 595. <https://doi.org/10.1038/msb.2012.28>
- Callahan, B. J., McMurdie, P. J., Rosen, M. J., Han, A. W., Johnson, A. J. A., & Holmes, S. P. (2016). DADA2: High-resolution sample inference
from Illumina amplicon data. *Nature Methods*, 13(7), 581–583. <https://doi.org/10.1038/nmeth.3869>
- Cameron, E. S., Schmidt, P. J., Tremblay, B. J. M., Emelko, M. B., & Müller, K. M. (2021). Enhancing diversity analysis by repeatedly rarefying next
generation sequencing data describing microbial communities. *Scientific Reports*, 11(1), 22302. <https://doi.org/10.1038/s41598-021-01636-1>
- Capo, E., Giguet-Covex, C., Rouillard, A., Nota, K., Heintzman, P. D., Vuillemin, A., et al. (2021). Lake sedimentary DNA research on past
terrestrial and aquatic biodiversity: Overview and recommendations. *Quaternary*, 4(1), 6. <https://doi.org/10.3390/quat4010006>
- Capo, E., Monchamp, M.-E., Coolen, M. J. L., Domaizon, I., Armbrecht, L., & Bertilsson, S. (2022). Environmental paleomicrobiology: Using DNA
preserved in aquatic sediments to its full potential. *Environmental Microbiology*, 24(5), 2201–2209. <https://doi.org/10.1111/1462-2920.15913>
- Cho, H., Hwang, C. Y., Kim, J.-G., Kang, S., Knittel, K., Choi, A., et al. (2020). A unique benthic microbial community underlying the *Phaeocys-
tis antarctica*-dominated Amundsen Sea Polynya, Antarctica: A proxy for assessing the impact of global changes. *Frontiers in Marine Science*,
6, 797. <https://doi.org/10.3389/fmars.2019.00797>
- Clarke, E. L., Taylor, L. J., Zhao, C., Connell, A., Lee, J.-J., Fett, B., et al. (2019). Sunbeam: An extensible pipeline for analyzing metagenomic
sequencing experiments. *Microbiome*, 7(1), 46. <https://doi.org/10.1186/s40168-019-0658-x>
- Clarke, L. J., Suter, L., Deagle, B. E., Polanowski, A. M., Terauds, A., Johnstone, G. J., & Stark, J. S. (2021). Environmental DNA metabarcoding
for monitoring metazoan biodiversity in Antarctic nearshore ecosystems. *PeerJ*, 9, e12458. <https://doi.org/10.7717/peerj.12458>
- Constable, A. J., Melbourne-Thomas, J., Corney, S. P., Arrigo, K. R., Barbraud, C., Barnes, D. K., et al. (2014). Climate change and Southern
Ocean ecosystems I: How changes in physical habitats directly affect marine biota. *Global Change Biology*, 20(10), 3004–3025. <https://doi.org/10.1111/gcb.12623>
- Corinaldesi, C., Dell'Anno, A., & Danovaro, R. (2007). Viral infection plays a key role in extracellular DNA dynamics in marine anoxic systems.
Limnology & Oceanography, 52(2), 508–516. <https://doi.org/10.4319/lno.2007.52.2.0508>
- Cowart, D. A., Murphy, K. R., & Cheng, C. H. C. (2018). Metagenomic sequencing of environmental DNA reveals marine faunal assemblages
from the West Antarctic Peninsula. *Marine Genomics*, 37, 148–160. <https://doi.org/10.1016/j.margen.2017.11.003>
- Creac'h, L., Noble, T. L., Chase, Z., Charlier, B. L. A., Townsend, A. T., Perez-Tribouillier, H., & Dietz, C. (2023). Unradiogenic reactive phase
controls the ϵ Nd of authigenic phosphates in East Antarctic margin sediment. *Geochimica et Cosmochimica Acta*, 344, 190–206. <https://doi.org/10.1016/j.gca.2023.01.001>
- Delmont, T. O., Kiefl, E., Kilinc, O., Esen, O. C., Uysal, I., Rappé, M. S., et al. (2019). Single-amino acid variants reveal evolutionary processes
that shape the biogeography of a global SAR11 subclade. *eLife*, 8, e46497. <https://doi.org/10.7554/eLife.46497>
- De Schepper, S., Ray, J. L., Skaar, K. S., Sadatzki, H., Ijaz, U. Z., Stein, R., & Larsen, A. (2019). The potential of sedimentary ancient DNA for
reconstructing past sea ice evolution. *The ISME Journal*, 13(10), 2566–2577. <https://doi.org/10.1038/s41396-019-0457-1>
- Dorschel, B., Hehemann, L., Viquerat, S., Warnke, F., Dreutter, S., Schulze Tenberge, Y., et al. (2022). The International Bathymetric Chart of
the Southern Ocean version 2 (IBCSO v2). *PANGAEA*. <https://doi.org/10.1594/PANGAEA.937574>
- Ewels, P., Magnusson, M., Lundin, S., & Källér, M. (2016). MultiQC: Summarize analysis results for multiple tools and samples in a single report.
Bioinformatics, 32(19), 3047–3048. <https://doi.org/10.1093/bioinformatics/btw354>
- Fetterer, F., Knowles, K., Meier, W. N., Savoie, M., & Windnagel, A. K. (2017). *Sea Ice Index, Version 3*. [G02135]. National Snow and Ice Data
Center. <https://doi.org/10.7265/NSK072F8>
- Fontanez, K. M., Eppley, J. M., Samo, T. J., Karl, D. M., & DeLong, E. F. (2015). Microbial community structure and function on sinking parti-
cles in the North Pacific Subtropical Gyre. *Frontiers in Microbiology*, 6, 469. <https://doi.org/10.3389/fmicb.2015.00469>
- Garlapati, D., Charankumar, B., Ramu, K., Madeswaran, P., & Murthy, R. (2019). A review on the applications and recent advances in envi-
ronmental DNA (eDNA) metagenomics. *Reviews in Environmental Science and Biotechnology*, 18(3), 389–411. <https://doi.org/10.1007/s11157-019-09501-4>
- Giguet-Covex, C., Ficetola, G. F., Walsh, K., Poulenard, J., Bajard, M., Fouinat, L., et al. (2019). New insights on lake sediment DNA from the
catchment: Importance of taphonomic and analytical issues on the record quality. *Scientific Reports*, 9(1), 14676. <https://doi.org/10.1038/s41598-019-50339-1>
- Gionfriddo, C., Tate, M., Wick, R., Schultz, M. B., Zemla, A., Thelen, M. P., et al. (2016). Microbial mercury methylation in Antarctic sea ice.
Nature Microbiology, 1(10), 16127. <https://doi.org/10.1038/nmicrobiol.2016.127>
- Giosan, L., Orsi, W. D., Coolen, M., Wuchter, C., Dunlea, A. G., Thirumalai, K., et al. (2018). Neoglacial climate anomalies and the Harappan
metamorphosis. *Climate of the Past*, 14(11), 1669–1686. <https://doi.org/10.5194/cp-14-1669-2018>
- Giovannoni, S. J. (2017). SAR11 bacteria: The most abundant plankton in the oceans. *Annual Review of Marine Science*, 9(1), 231–255. <https://doi.org/10.1146/annurev-marine-010814-015934>
- Godhe, A., Asplund, M. E., Härnström, K., Saravanan, V., Tyagi, A., & Karunasagar, I. (2008). Quantification of diatom and dinoflagellate
biomasses in coastal marine seawater samples by real-time PCR. *Applied and Environmental Microbiology*, 74(23), 7174–7182. <https://doi.org/10.1128/aem.01298-08>
- Greenbaum, J. S., Blankenship, D. D., Young, D. A., Richter, T. G., Roberts, J. L., Aitken, A. R. A., et al. (2015). Ocean access to a cavity beneath
Totten Glacier in East Antarctica. *Nature Geoscience*, 8(4), 294–298. <https://doi.org/10.1038/ngeo2388>
- Guidi, L., Chaffron, S., Bittner, L., Eveillard, D., Larhlimi, A., Roux, S., et al. (2016). Plankton networks driving carbon export in the oligotrophic
ocean. *Nature*, 532(7600), 465–470. <https://doi.org/10.1038/nature16942>
- Heaton, T. J., Köhler, P., Butzin, M., Bard, E., Reimer, R. W., Austin, W. E. N., et al. (2020). Marine20—The marine radiocarbon age calibration
curve (0–55,000 Cal BP). *Radiocarbon*, 62(4), 779–820. <https://doi.org/10.1017/rdc.2020.68>
- Herbig, A., Maixner, F., Bos, K. I., Zink, A., Krause, J., & Huson, D. H. (2016). MALT: Fast alignment and analysis of metagenomic DNA
sequence data applied to the Tyrolean Iceman. *bioRxiv*. <https://doi.org/10.1101/050559>
- Holder, L., Duffy, M., Opdyke, B., Leventer, A., Post, A., O'Brien, P., & Armand, L. K. (2020). Controls since the mid-Pleistocene transi-
tion on sedimentation and primary productivity downslope of Totten Glacier, East Antarctica. *Paleoceanography and Paleoclimatology*, 35,
e2020PA003981. <https://doi.org/10.1029/2020PA003981>
- Huson, D. H., Beier, S., Flade, I., Görska, A., El-Hadidi, M., Mitra, S., et al. (2016). MEGAN community edition—Interactive exploration
and analysis of large-scale microbiome sequencing data. *PLoS Computational Biology*, 12(6), e1004957. <https://doi.org/10.1371/journal.pcbi.1004957>

- Imachi, H., Tasumi, E., Takaki, Y., Hoshino, T., Schubotz, F., Gan, S., et al. (2019). Cultivable microbial community in 2-km-deep, 20-million-year-old seafloor coalbeds through ~1000 days anaerobic bioreactor cultivation. *Scientific Reports*, 9(1), 2305. <https://doi.org/10.1038/s41598-019-38754-w>
- Inagaki, F., Hinrichs, K. U., Kubo, Y., Bowles, M. W., Heuer, V. B., Hong, W. L., et al. (2015). Exploring deep microbial life in coal-bearing sediment down to ~2.5 km below the ocean floor. *Science*, 349(6246), 420–424. <https://doi.org/10.1126/science.aaa6882>
- Inagaki, F., Nunoura, T., Nakagawa, S., Teske, A., Lever, M., Lauer, A., et al. (2006). Biogeographical distribution and diversity of microbes in methane hydrate-bearing deep marine sediments on the Pacific Ocean Margin. *Proceedings of the National Academy of Sciences of the United States of America*, 103(8), 2815–2820. <https://doi.org/10.1073/pnas.0511033103>
- IPCC. (2021). Summary for policymakers. In V. Masson-Delmotte, et al. (Eds.), *Climate change 2021: The physical science basis. Contribution of Working Group I to the sixth assessment report of the Intergovernmental Panel on Climate Change* (pp. 3–32). Cambridge University Press. <https://doi.org/10.1017/9781009157896.001>
- Ishitani, Y., Ujiié, Y., de Vargas, C., Not, F., & Takahashi, K. (2012). Phylogenetic relationships and evolutionary patterns of the order Collodaria (Radiolaria). *PLoS One*, 7(5), e35775. <https://doi.org/10.1371/journal.pone.0035775>
- Kawaguchi, S., Kurihara, H., King, R., Hale, L., Berli, T., Robinson, J. P., et al. (2011). Will krill fare well under Southern Ocean acidification? *Biology Letters*, 7(2), 288–291. <https://doi.org/10.1098/rsbl.2010.0777>
- Learman, D. R., Henson, M. W., Thrash, J., Cameron, T. B., Brannock, P. M., Santos, S. R., et al. (2016). Biogeochemical and microbial variation across 5500 km of Antarctic surface sediment implicates organic matter as a driver of benthic community structure. *Frontiers in Microbiology*, 7, 284. <https://doi.org/10.3389/fmicb.2016.00284>
- Leventer, A. (2022). Quantitative diatom data collected from the 2017 RV *Investigator* voyage, IN2017_V01 [Dataset]. Australian Antarctic Data Centre. <https://doi.org/10.26179/5cad45a7cb140>
- Li, X., Rignot, E., Morlighem, M., Mouginit, J., & Scheuchl, B. (2015). Grounding line retreat of Totten Glacier, East Antarctica, 1996 to 2013: Totten Glacier grounding line retreat. *Geophysical Research Letters*, 42, 8049–8056. <https://doi.org/10.1002/2015GL065701>
- Lin, Y., Moreno, C., Marchetti, A., Ducklow, H., Schofield, O., Delage, E., et al. (2021). Decline in plankton diversity and carbon flux with reduced sea ice extent along the Western Antarctic Peninsula. *Nature Communications*, 12(1), 4948. <https://doi.org/10.1038/s41467-021-25235-w>
- Lougheed, B. C., & Obrochta, S. P. (2016). MatCal: Open source Bayesian ¹⁴C age calibration in Matlab. *Journal of Open Research Software*, 4, 1–4.
- Martin, M. (2011). Cutadapt removes adapter sequences from high-throughput sequencing reads. *EMBnet journal*, 17(1), 10–12. <https://doi.org/10.14806/ej.17.1.200>
- McLeod, D. J., Hallegraeff, G. M., Hosie, G. W., & Richardson, A. J. (2012). Climate-driven range expansion of the red-tide dinoflagellate *Noctiluca scintillans* into the Southern Ocean. *Journal of Plankton Research*, 34(4), 332–337. <https://doi.org/10.1093/plankt/fbr112>
- McMurdie, P. J., & Holmes, S. (2013). phyloseq: An R package for reproducible interactive analysis and graphics of microbiome census data. *PLoS One*, 8(4), e61217. <https://doi.org/10.1371/journal.pone.0061217>
- Meyer, M., & Kircher, M. (2010). Illumina sequencing library preparation for highly multiplexed target capture and sequencing. *Cold Spring Harbour Protocols*, 2010(6), 5448. <https://doi.org/10.1101/pdb.prot5448>
- Morris, R. M., Longnecker, K., & Giovannoni, S. J. (2006). *Pirellula* and OM43 are among the dominant lineages identified in an Oregon coast diatom bloom. *Environmental Microbiology*, 8, 1361–1370. <https://doi.org/10.1111/j.1462-2920.2006.01029.x>
- Morris, R. M., Rappé, M. S., Vergin, K. L., Siebold, W. A., Carlson, C. A., & Giovannoni, S. J. (2002). SAR11 clade dominates ocean surface bacterioplankton communities. *Nature*, 420(6917), 806–810. <https://doi.org/10.1038/nature01240>
- O'Brien, P. E., Post, A. L., Edwards, S., Martin, T., Caburlotto, A., Donda, F., et al. (2020). Continental slope and rise geomorphology seaward of the Totten Glacier, East Antarctica (112°E–122°E). *Marine Geology*, 427, 106221. <https://doi.org/10.1016/j.margeo.2020.106221>
- Oksanen, A. J., Blanchet, F. G., Kindt, R., Legendre, P., Minchin, P. R., & Hara, R. B. O. (2020). vegan: Community Ecology Package (R package version 2.5-7). Retrieved from <https://cran.r-project.org/package=vegan>
- Orsi, W. D., Coolen, M., Wuchter, C., He, L., More, K. D., Irigoien, X., et al. (2017). Climate oscillations reflected within the microbiome of Arabian Sea sediments. *Scientific Reports*, 7, 6040. <https://doi.org/10.1038/s41598-017-05590-9>
- Paulson, J. N., Stine, O. C., Bravo, H. C., & Pop, M. (2013). Differential abundance analysis for microbial marker-gene surveys. *Nature Methods*, 10(12), 1200–1202. <https://doi.org/10.1038/nmeth.2658>
- Pawlowska, J., Lejzerowicz, F., Esling, P., Szczuciński, W., Zajaczkowski, M., & Pawlowski, J. (2014). Ancient DNA sheds new light on the Svalbard foraminiferal fossil record of the last millennium. *Geobiology*, 12(4), 277–288.
- Pawlowska, J., Wollenburg, J. E., Zajaczkowski, M., & Pawlowski, J. (2020). Planktonic foraminifera genomic variations reflect paleoceanographic changes in the Arctic: Evidence from sedimentary ancient DNA. *Scientific Reports*, 10(1), 15102. <https://doi.org/10.1038/s41598-020-72146-9>
- Pernice, M., Giner, C., Logares, R., Perera-Bel, J., Acinas, S. G., Duarte, C. M., et al. (2016). Large variability of bathypelagic microbial eukaryotic communities across the world's oceans. *The ISME Journal*, 10(4), 945–958. <https://doi.org/10.1038/ismej.2015.170>
- Post, A. L., Lavoie, C., Domack, E. W., Leventer, A., Shevenell, A., & Fraser, A. D. (2017). Environmental drivers of benthic communities and habitat heterogeneity on an East Antarctic shelf. *Antarctic Science*, 29(1), 17–32. <https://doi.org/10.1017/s0954102016000468>
- Post, A. L., O'Brien, P. E., Edwards, S., Carroll, A. G., Malakoff, K., & Armand, L. K. (2020). Upper slope processes and seafloor ecosystems on the Sabrina continental slope, East Antarctica. *Marine Geology*, 422, 106091. <https://doi.org/10.1016/j.margeo.2019.106091>
- Raiswell, R., Hawkings, J. R., Benning, L. G., Baker, A. R., Death, R., Albani, S., et al. (2016). Potentially bioavailable iron delivery by iceberg-hosted sediments and atmospheric dust to the polar oceans. *Biogeosciences*, 13, 3887–3900. <https://doi.org/10.5194/bg-13-3887-2016>
- R Core Team. (2020). *R: A language and environment for statistical computing*. R Foundation for Statistical Computing. Retrieved from <https://www.R-project.org/>
- Rignot, E., Mouginit, J., Scheuchl, B., van den Broeke, M., van Wessem, M. J., & Morlighem, M. (2019). Four decades of Antarctic Ice Sheet mass balance from 1979–2017. *Proceedings of the National Academy of Sciences of the United States of America*, 116(4), 1095–1103. <https://doi.org/10.1073/pnas.1812883116>
- Rogers, A. D., Frinault, B. A. V., Barnes, D. K. A., Bindoff, N. L., Downie, R., Ducklow, H. W., et al. (2020). Antarctic futures: An assessment of climate-driven changes in ecosystem structure, function, and service provisioning in the Southern Ocean. *Annual Review of Marine Science*, 12(1), 87–120. <https://doi.org/10.1146/annurev-marine-010419-011028>
- Rohling, E., Grant, K., Hemleben, C., Siddall, M., Hoogakker, B. A. A., Bolshaw, M., & Kucera, M. (2008). High rates of sea-level rise during the Last Interglacial period. *Nature Geoscience*, 1, 38–42. <https://doi.org/10.1038/ngeo.2007.28>
- Schubert, M., Lindgreen, S., & Orlando, L. (2016). AdapterRemoval v2: Rapid adapter trimming, identification, and read merging. *BMC Research Notes*, 9(1), 88. <https://doi.org/10.1186/s13104-016-1900-2>

- Selway, C. A., Armbrrecht, L., & Thornalley, D. (2022). An outlook for the acquisition of marine sedimentary ancient DNA (*seDNA*) from North Atlantic Ocean archive material. *Paleoceanography and Paleoclimatology*, 37, e2021PA004372. <https://doi.org/10.1029/2021PA004372>
- Silvano, A., Rintoul, S. R., Kusahara, K., Peña-Molino, B., van Wijk, E., Gwyther, D. E., & Williams, G. D. (2019). Seasonality of warm water intrusions onto the continental shelf near the Totten Glacier. *Journal of Geophysical Research: Oceans*, 124, 4272–4289. <https://doi.org/10.1029/2018JC014634>
- Skinner, L. C., Muschitiello, F., & Scrivner, A. E. (2019). Marine reservoir age variability over the last deglaciation: Implications for marine carbon cycling and prospects for regional radiocarbon calibrations. *Paleoceanography and Paleoclimatology*, 34, 1807–1815. <https://doi.org/10.1029/2019PA003667>
- Slon, V., Hopfe, C., Weiß, C. L., Mafessoni, F., De la Rasilla, M., Lalueza-Fox, C., et al. (2017). Neandertal and Denisovan DNA from Pleistocene sediments. *Science*, 356(6338), 605–608. <https://doi.org/10.1126/science.aam9695>
- Thomsen, P. F., & Willerslev, E. (2015). Environmental DNA—An emerging tool in conservation for monitoring past and present biodiversity. *Biological Conservation*, 183, 4–18. <https://doi.org/10.1016/j.biocon.2014.11.019>
- Tooze, S., Halpin, J. A., Noble, T. L., Chase, Z., O'Brien, P. E., & Armand, L. (2020). Scratching the surface: A marine sediment provenance record from the continental slope of central Wilkes Land, East Antarctica. *Geochemistry, Geophysics, Geosystems*, 21, e2020GC009156. <https://doi.org/10.1029/2020GC009156>
- Wang, Q., Garrity, G. M., Tiedje, J. M., & Cole, J. R. (2007). Naive Bayesian classifier for rapid assignment of rRNA sequences into the new bacterial taxonomy. *Applied and Environmental Microbiology*, 73(16), 5261–5267. <https://doi.org/10.1128/aem.00062-07>
- Warnock, J. P., & Scherer, R. P. (2015). A revised method for determining the absolute abundance of diatoms. *Journal of Paleolimnology*, 53(1), 157–163. <https://doi.org/10.1007/s10933-014-9808-0>
- Wei, W., Chen, X., Weinbauer, M. G., Jiao, N., & Zhang, R. (2022). Reduced bacterial mortality and enhanced viral productivity during sinking in the ocean. *The ISME Journal*, 16(6), 1668–1675. <https://doi.org/10.1038/s41396-022-01224-9>
- Wickham, H., Averick, M., Bryan, J., Chang, W., McGowan, L., François, R., et al., (2019). Welcome to the tidyverse. *Journal of Open Source Software*, 4(43), 1686. <https://doi.org/10.21105/joss.01686>
- Wilkins, D., Lauro, F. M., Williams, T. J., Demaere, M. Z., Brown, M. V., Hoffman, J. M., et al. (2013). Biogeographic partitioning of Southern Ocean microorganisms revealed by metagenomics. *Environmental Microbiology*, 15(5), 1318–1333. <https://doi.org/10.1111/1462-2920.12035>
- Williams, T. J., Wilkins, D., Long, E., Evans, F. F., DeMaere, M. Z., Raftery, M. J., & Cavicchioli, R. (2013). The role of planktonic Flavobacteria in processing algal organic matter in coastal East Antarctica revealed using metagenomics and metaproteomics. *Environmental Microbiology*, 15(5), 1302–1317. <https://doi.org/10.1111/1462-2920.12017>
- Wright, K. (2021). pals: Color palettes, colormaps, and tools to evaluate them. Retrieved from <https://CRAN.R-project.org/package=pals>
- Zhou, M. Y., Wang, G. L., Li, D., Zhao, D. L., Qin, Q. L., Chen, X. L., et al. (2013). Diversity of both the cultivable protease-producing bacteria and bacterial extracellular proteases in the coastal sediments of King George Island, Antarctica. *PLoS One*, 8(11), e79668. <https://doi.org/10.1371/journal.pone.0079668>
- Zhou, Z., Tran, P. Q., Kieft, K., & Anantharaman, K. (2020). Genome diversification in globally distributed novel marine proteobacteria is linked to environmental adaptation. *The ISME Journal*, 14(8), 2060–2077. <https://doi.org/10.1038/s41396-020-0669-4>
- Zimmermann, H. H., Stooß-Leichsenring, K. R., Kruse, S., Müller, J., Stein, R., Tiedemann, R., & Herzschuh, U. (2020). Changes in the composition of marine and sea-ice diatoms derived from sedimentary ancient DNA of the eastern Fram Strait over the past 30,000 years. *Ocean Science*, 16(5), 1017–1032. <https://doi.org/10.5194/os-16-1017-2020>
- Zimmermann, H. H., Stooß-Leichsenring, K. R., Kruse, S., Nürnberg, D., Tiedemann, R., & Herzschuh, U. (2021). Sedimentary ancient DNA from the subarctic North Pacific: How sea ice, salinity, and insolation dynamics have shaped diatom composition and richness over the past 20,000 years. *Paleoceanography and Paleoclimatology*, 36, e2020PA004091. <https://doi.org/10.1029/2020PA004091>

References From the Supporting Information

- Urlich, M. A., Nery, J. R., Lister, R., Schmitz, R. J., & Ecker, J. R. (2015). MethylC-seq library preparation for base-resolution whole-genome bisulfite sequencing. *Nature Protocols*, 10(3), 475–483. <https://doi.org/10.1038/nprot.2014.114>